博士論文

Analysis of the host responses to influenza virus infection and their application to the development of vaccines

（インフルエンザウイルスに対する宿主応答の解析とワクチン開発への応用）

桂　廣亮

CONTENTS

PREFACE

On account of the affluence and medical advances of developed countries, we now have an average life expectancy of 80 years. Then, the risk of various diseases such as cancers, cardiac disorders, apoplexy, and diabetes increases. Meanwhile, infectious diseases have been a threat to all mankind regardless of age and sex since time began. Influenza is one of the most familiar infectious diseases. It is a respiratory disorder caused by influenza viruses. Influenza can cause severe clinical symptoms compared with other respiratory infectious diseases, and it is highly contagious. Accordingly, the influenza virus is a considerable burden on medical and public health worldwide.

Influenza viruses belong to the *Orthomyxoviridae* family and possess eight segments of negative-stranded viral RNA (vRNA). They are classified into three major types, influenza A, B, and C viruses, based on the antigenicities of their internal proteins (Wright et al., 2013). Influenza A and B viruses have been circulating in humans. Because influenza A viruses have the potential to cause pandemics, these viruses have been extensively studied from global surveillance to their interactions with host cell systems.

Influenza A viruses are further classified into subtypes based on the antigenicities of their two surface proteins, hemagglutinin (HA) and neuraminidase (NA). Currently, 18 HA and 9 NA subtypes have been identified (Tong et al., 2012; Tong et al., 2013; Wright et al., 2013). During the 20th century, we experienced three pandemics caused by influenza A virus: Spanish influenza in 1918 (H1N1 subtype), Asian influenza in 1957 (H2N2 subtype), and Hong Kong influenza in 1968 (H3N2 subtype). Although the origin of the Spanish influenza remains controversial, the H2 HA, N2 NA, and PB1 gene segments of the Asian influenza and the H3 HA and PB1 gene segments of the Hong

1

Kong influenza came from avian influenza viruses (Scholtissek et al., 1978; Kawaoka et al., 1989). In 2009, the newly emerging swine origin influenza A virus (H1N1) rapidly spread all over the world and resulted in the first pandemic of this century. The World Health Organization (WHO) defined this virus as A(H1N1) pdm09. At that time, a triple reassortant virus between human H3N2, North American avian, and classical swine viruses was circulating in the North American pig population. A(H1N1) pdm09 emerged by further reassortment of the triple reassortant virus with a Eurasian avian-like swine virus (Dawood et al., 2009; Smith et al., 2009). Thus, newly emerging viruses that result from the reassortment of viral gene segments derived from distinct viruses circulating in various animals can occasionally cause pandemics. This is a key characteristic of influenza viruses.

Since the first case of human infection with an H5N1 highly pathogenic avian influenza virus was identified in Hong Kong in 1997 (Claas et al., 1998), H5N1 viruses have undergone rigorous surveillance. Avian influenza viruses are thought to have a low probability of airborne human-to-human transmission due, in part, to the difference in receptor binding preference between human and avian viruses (Rogers et al., 1983); indeed, only sporadic cases of infection have been reported. Nevertheless, the case fatality rate of infection with H5N1 highly pathogenic avian influenza viruses is estimated to be ~60%. Therefore, a pandemic caused by one of these viruses would inflict enormous damage on human society. Recently, several mutations in H5 HA that allow transmission between mammals via the airborne route were identified in a ferret model (Herfst et al., 2012; Imai et al., 2012). Importantly, H5N1 avian influenza viruses that possess some of these mutations have been isolated in nature (Neumann et al., 2012).

In addition to H5N1 subtypes, H7N9 avian influenza virus infection of humans

was reported in China in 2013 (Chen et al., 2013; Gao et al., 2013; Li et al., 2013). Because viruses of the H7N9 subtype have not previously circulated in humans, no one has specific immunity against these viruses (Watanabe et al., 2013). To make matters worse, limited transmissibility of H7N9 viruses isolated from human patients was observed in a ferret model (Belser et al., 2013; Richard et al., 2013; Watanabe et al., 2013). If influenza viruses we have never encountered acquire the ability to transmit more readily via the airborne route from person to person, it is highly likely that such viruses will cause a pandemic. It is difficult to predict which subtype of virus will cause a pandemic; therefore, we have to continue the global surveillance and basic research of influenza viruses.

Influenza viruses infect the respiratory tract. Avian influenza viruses preferentially recognize α2,3-linked sialic acid (SA) and human isolates recognize α2,6-linked SA as receptors (Rogers et al., 1983). After binding and internalization, viruses are transported via the endocytosis pathway (Matlin et al., 1981; Sieczkarski et al., 2002), and then viral RNAs (vRNAs) are released from virions after virus-host membrane fusion. During the influenza virus replication cycle, vRNAs are sensed by pattern recognition receptors (PRRs), such as retinoic acid inducible gene-I (RIG-I) (Hornung et al., 2004; Pichlmair et al., 2004) and toll-like receptor (TLR) 7 (Diebold et al., 2004), and subsequent antiviral responses, including the production of type I interferon, pro-inflammatory cytokines, and chemokines, are elicited (Kawai et al., 2006). Then, various immune cells such as monocytes and neutrophils infiltrate the sites of infection depending on the secreted chemokines to contain the spread of virus and remove the virus-infected cells. The inflammatory responses then resolve due to the action of anti-inflammatory cytokines such as interleukin (IL)-10, and adaptive immunity, which is dominated by T cells and B cells, is activated. In this doctoral thesis, I focused on three points: (1)

influenza virus infection within host cells and the induction of antiviral responses *in vivo*, (2) the resolution of inflammation, and (3) the induction of virus-specific adaptive immunity.

Little is known about how an influenza virus infection spreads throughout the body over time due to the lack of a suitable reporter virus that would allow us to detect virus-infected cells easily in the body. It is difficult to stably express a foreign gene because the size of the viral genome is limited and the mechanisms for incorporation of segmented viral genomes into virions are not fully understood. In 2010, a replication-competent recombinant virus that expressed green fluorescent protein (GFP) in infected cells was reported (Manicassamy et al., 2010). This reporter virus was very useful, but had several problems in terms of stability of GFP expression. For these reasons, our group improved the expression of the fluorescent protein in this reporter virus. In chapter I, I will describe the characterization of the improved reporter virus and my analysis of the host responses obtained when using this reporter virus.

To prevent infection with influenza viruses, vaccination is one of the most effective measures. Two types of influenza vaccines are available, inactivated vaccines and live attenuated vaccines; however, there is still room for improvement in terms of their immunogenicity and safety, respectively (Cox et al., 2004). In chapter II, I show the results of my assessment of the efficacy of a new vaccine based on a replication-incompetent virus. Specifically, I generated a replication-incompetent virus that was deficient in HA membrane fusion activity and assessed its vaccine efficacy.

In chapter III, I attempted to develop a bivalent vaccine based on a replication-incompetent virus that carried an antigen for another respiratory infectious agent, *Streptococcus pneumoniae*. I selected *S. pneumoniae* because it is a causative agent of

not only community-acquired pneumonia but also a bacterial pneumonia that follows influenza virus infection (Morens et al., 2008; Jambo et al., 2010; Gill et al., 2010). I generated a virus that expresses pneumococcal surface protein A (PspA) in infected cells, and then assessed its vaccine efficacy in mice. I conclude my thesis by suggesting new possibilities for replication-incompetent viruses.

CHAPTER I

Characterization of a recombinant influenza A virus carrying the Venus gene and its application for the analysis of the infection dynamics in the mouse lung.

Abstract

   Reporter viruses that possess the genes for reporter proteins are useful to
explore the dynamics of influenza virus infection *in vivo*. Recently, a replication-
competent recombinant influenza A virus carrying the gene for green fluorescent protein
(GFP) was reported. Although this recombinant virus was useful to detect virus-infected
cells by flow cytometry, some improvements were required to use the virus for live
imaging experiments due to the instability of GFP expression and low replication
ability. To overcome these issues, our group generated a similar recombinant virus
(NS1-Venus PR8 WT) possessing the Venus gene instead of the GFP gene for the
fluorescent protein, serially passed it *in vivo* and *in vitro*, then I analyzed its properties.
After passage in mice, this virus (NS1-Venus PR8 MA) replicated to a similar level to
that of the wild-type virus, and Venus expression was strong in the mice lung. Two
amino acid substitutions were found in PB2 and HA after passage. The level of Venus
expression was augmented by the PB2-E712D mutation. In addition, the threshold of
the pH range for fusion was increased by the HA-T380A mutation. These mutations
resulted in potent Venus expression and efficient viral replication. Since virus-infected
cells could be observed easily by using NS1-Venus PR8 MA, I used them to observe
virus-infected cells in whole lung lobe in combination with the transparent reagent
SCALEVIEW A2. Finally, I assessed the effects of virus infection on the function of
monocytes and alveolar macrophages by using microarray analysis. I found that the
expression of several cytokines including type I interferons and chemokines was
augmented in virus-infected monocytes and alveolar macrophages. In addition, the
genes involved in the response to wounding were also up-regulated in these cells. Taken
together, I demonstrated that NS1-Venus PR8 MA possesses high growth ability and

strong Venus expression in infected cells due to mutations acquired during mouse passage, suggesting that NS1-Venus PR8 MA could be widely applicable in many experimental settings.

Introduction

Influenza viruses are causative pathogens of contagious respiratory disease, causing annual epidemics, which impact economic and public health. In addition to seasonal influenza, pandemics caused by newly emerging viruses are also a concern. In 2009, swine-origin H1N1 influenza A virus caused the first pandemic of this century. This virus rapidly encompassed the entire globe, and vast number of infections were reported (http://www.who.int/csr/don/2010_08_06/en/index.html). Given the clear threat of influenza viruses to human health, strenuous efforts have been made to develop new antivirals and vaccines against these viruses.

An understanding of the dynamics of influenza virus infection inside the body is essential to evaluate the pathogenicity of influenza virus or the efficacy of antivirals and vaccines. To analyze the dynamics of influenza virus infection *in vivo*, a reporter virus carrying the gene for a fluorescent protein [e.g. green fluorescent protein (GFP)] is useful. Previously, we and others developed several reporter viruses possessing the GFP gene instead of the nonstructural (NS) 1 gene or the neuraminidase (NA) gene (Shinya et al., 2004; Kittel et al., 2004). These viruses can infect host cells and express both GFP and viral proteins in the infected cells. However, because their replication is strongly impaired in wild-type mice, these viruses are unsuitable for use in *in vivo* experiments. Recently, Manicassamy et al. (2010) successfully generated a recombinant virus that possessed the GFP gene in its NS segment and expressed an NS1-GFP fusion protein in infected cells. This virus could replicate *in vitro* and *in vivo*, and exhibit pathogenicity in BALB/c mice, although it was attenuated compared with wild-type PR8 virus. This virus was a clear advancement; however, the GFP signal was weak in lung sections and GFP expression was not stable during virus replication.

9

To overcome these disadvantages, our group improved the NS1-GFP virus. We generated a recombinant virus that possesses Venus as the fluorescent protein instead of GFP in the same manner as the NS1-GFP virus that Manicassamy et al. produced. Venus is a variant of yellow fluorescent protein (YFP) and is brighter than GFP (Nagai et al., 2002). To increase the pathogenicity of NS1-Venus virus, we serially passaged it in mice and culture cells. After these passages, we found that this mouse-adapted NS1-Venus PR8 virus was virulent in mice and exhibited high Venus expression *in vitro* and *in vivo*. Here, I describe the characterization of this virus and demonstrate how influenza virus spreads throughout the lung by using mouse-adapted NS1-Venus PR8-infected lungs that were made transparent with SCALEVIEW A2 (Hama et al., 2011). Further, I identified the target cells of influenza virus by means of an immunofluorescence assay and flow cytometry. In addition, to understand the host responses in lungs, I performed microarray analysis to explore transcriptomes of Venus-positive and -negative monocytes and alveolar macrophages in lungs from mice infected with NS1-Venus PR8 MA.

In summary, I generated NS1-Venus PR8 MA, which has improved expression levels of Venus, which, in turn, allowed me to detect virus-infected cells *in vivo* more clearly and easily, and to conduct detailed analyses of individual infected cells. This reporter virus could have various applications for influenza research.

Materials and Methods

Cells and viruses. Madin-Darby canine kidney (MDCK) cells were maintained in minimum essential medium (MEM) containing 5% of newborn calf serum (NCS). Human embryonic kidney 293T (HEK293T) and HEK293 cells were maintained in Dulbecco's modified Eagle medium supplemented with 10% fetal calf serum (FCS). A/Puerto Rico/8/34 (H1N1; PR8) (Horimoto et al., 2007) and each NS1-Venus PR8 virus were generated by using reverse genetics and were propagated in MDCK cells at 37°C for 48 h in MEM containing L-(tosylamido-2-phenyl) ethyl chloromethyl ketone (TPCK) -treated trypsin (0.8 μg/ml) and 0.3% bovine serum albumin (BSA) (Sigma Aldrich).

Adaptation of NS1-Venus PR8 virus in mice. Six- to eight-week-old female C57BL/6 mice (Japan SLC) were intranasally infected with 50 μl of 2.3×10^6 plaque-forming units (PFU) of NS1-Venus PR8 virus. Lungs were harvested 3–6 days post-infection (dpi) and homogenized in 1 ml of phosphate-buffered saline (PBS). To obtain a clone with high proliferative ability and Venus expression, plaque purification of the lung homogenate using MDCK cells was performed. A large, highly Venus-expressing plaque was picked and the cloned virus was propagated in MDCK cells at 37°C for 48 h, then 50 μl of the supernatant was used as an inoculum for the next passage. These procedures were repeated six times.

Sequence analysis. Sequence analysis of viral RNA was performed as described previously (Sakabe et al., 2011). Briefly, viral RNAs were extracted by using a QIAamp Viral RNA mini kit (QIAGEN) and Superscript III™ reverse transcriptase (Invitrogen)

11

and an oligonucleotide complementary to the 12-nucleotide sequence at the 3' end of the viral RNA (Katz et al., 1990) were used for reverse transcription of viral RNAs. Each segment was amplified by using PCR with Phusion High Fidelity DNA polymerase (Finnzymes) and primers specific for each segment of the PR8 virus. The PCR products were purified and their sequences determined by using ABI 3130xl (Applied Biosystems).

Plasmid construction and reverse genetics. Plasmids containing the cloned cDNAs of PR8 genes between the human RNA polymerase I promoter and the mouse RNA polymerase I terminator (referred to as PolI plasmid) were used for reverse genetics and as templates for mutagenesis. The mutations found in NS1-Venus PR8 virus after passage were introduced into the plasmid constructs of PR8 by using site-directed mutagenesis (referred to as pPolIR-PR8-PB2-E712D and pPolIR-PR8-HA-T380A, respectively). Reverse genetics was performed as described previously (Neumann et al., 1999). The eight PolI plasmids were cotransfected into HEK293T cells together with eukaryotic protein expressing plasmids for PB2, PB1, PA, and NP derived from PR8 by using the TransIT-293 transfection reagent (Mirus). Forty-eight hours after transfection, the supernatant was harvested and propagated once in MDCK cells at 37°C for 48 h in MEM containing TPCK-treated trypsin (0.8 μg/ml) and 0.3% BSA. Cell debris was removed by centrifugation at 2,100 x g for 20 min at 4°C, and the supernatants were stored at -80°C until use. The virus titers were determined by means of a plaque assay using MDCK cells.

Polykaryon formation assay. Polykaryon formation assay was performed as described previously (Imai et al., 2012) with modifications. HEK293 cells propagated in

24-well plates were infected with wild-type PR8 or PR8 possessing the hemagglutinin (HA) mutation found in NS1-Venus PR8 MA virus in DMEM containing 10% FCS at a multiplicity of infection (MOI) of 10. At 18 h post-infection, cells were washed with MEM containing 0.3% BSA and treated with TPCK-treated trypsin (1 µg/ml) in MEM containing 0.3% BSA for 15 min at 37°C to cleave the HA on the cell surface into HA1 and HA2. Trypsin was inactivated by washing the cells with DMEM containing 10% FCS. To initiate polykaryon formation, cells were exposed to low-pH buffer (145 mM NaCl, 20 mM sodium citrate (pH 6.0–5.4)) for 2 min at 37°C. Then the low-pH buffer was replaced with DMEM containing 10% FCS and the cells were incubated for 2 h at 37°C. The cells were then fixed with methanol and stained with Giemsa's solution. A microscope mounted with a digital camera (Nikon) was used to obtain photographic images.

Western blotting. MDCK cells were infected with each virus at an MOI of 1 without trypsin. The cells were lysed with Novex® Tris-Glycine SDS sample buffer (Invitrogen) 12 h after infection and subjected to SDS-polyacrylamide gel electrophoresis. Then, the proteins were transferred to a PVDF membrane in transfer buffer (100 mM Tris, 190 mM glycine). After membrane blocking, the membranes were incubated with a rabbit anti-GFP polyclonal antibody (MBL) or rabbit antiserum to A/WSN/33(H1N1)(R309), which was available in our laboratory. This antiserum reacts with influenza viral proteins including HA, NP, and matrix protein (M1). After incubation with the primary antibodies followed by washing with PBS containing 0.05% Tween-20 (PBS-T), the membranes were incubated with ECL™ anti-rabbit IgG HRP-linked whole antibody (GE Healthcare). Finally, specific proteins were detected by using the ECL Plus Western Blotting Detection

System (GE Healthcare). The VersaDoc Imaging System (Bio-Rad) was used to obtain photographic images.

Pathogenicity and replication of viruses in mice. Six-week-old female C57BL/6 mice were intranasally infected with 50 μl of 10^3, 10^4 or 10^5 PFU of each virus. Four mice per group were monitored for survival and body weight changes for 14 days after infection. Three mice per group were infected with 10^3 PFU of each virus and euthanized on the indicated days. Their lungs were collected to determine viral titers by means of plaque assay on MDCK cells.

Immunofluorescence assay. Six-week-old female C57BL/6 mice were intranasally infected with 50 μl of 10^4 PFU of each virus. Three mice per group were euthanized on the indicated days. To fix the lungs, they were intratracheally injected with 800 μl of 4% paraformaldehyde (PFA) phosphate buffer solution and then removed. After incubation with 10 ml of 4% PFA at 4°C for 4 h, the buffer was replaced with 10%, 20%, and 30% sucrose in PBS in a stepwise fashion. Then lungs were embedded in Optimum Cutting Temperature (OCT) Compound (Tissue-Tek) and frozen in liquid nitrogen. Frozen sections (6 μm in thickness) were permeabilized in 0.2% Triton X-100 in PBS and incubated with primary antibodies at 4°C for 12 h. Primary antibodies were goat anti-Clara cell 10 kDa protein (CC10) (Santa Cruz, sc-9772), rabbit anti-surfactant protein C (SP-C) (Santa Cruz, sc-13979), golden Syrian hamster anti-podoplanin (eBioscience, eBio8.1.1), and rabbit anti-calcitonin gene-related peptide (CGRP) (Sigma-Aldrich, C8198). After being washed with PBS, the sections were incubated with species-specific fluorescence dye-conjugated secondary antibodies at room temperature for 30 min.

Nuclei were stained with Hoechst33342 (Invitrogen). A Nikon A1 confocal microscope (Nikon) was used to observe the sections.

Preparation of transparent samples. Transparent samples were prepared by using SCALEVIEW A2 (Olympus) in accordance with a previous report (Hama et al., 2012). Six-week-old female C57BL/6 mice were intranasally infected with 50 μl of 10^5 PFU of each virus. Intracardial perfusion was performed on the indicated days and lungs were fixed with 4% PFA in PBS for 4 h at 4°C. Lungs were incubated with 10%, 20%, and 30% sucrose in PBS as described above, embedded in OCT compound, and frozen in liquid nitrogen. After the samples were thawed and rinsed in PBS, they were fixed again with 4% PFA in PBS for 30 min at room temperature. Then the lungs were transferred to SCALEVIEW A2 and incubated at 4°C for at least 2 weeks. SCALEVIEW A2 was exchanged every 2–3 days. Transparent samples were observed by using a stereo fluorescence microscope (Leica M205FA) mounted with a digital camera (DFC365FX) and filter GFP 3 (480/40 LP510).

Flow cytometry. To prepare single-cell suspensions, lungs were minced with scissors and digested with 20 mg of collagenase D (Roche) and 200 units of DNase (Worthington) for 30 min at 37°C. Samples were then passed through 100-μm cell strainers and red blood cells were lysed by red blood cell lysis buffer (Sigma Aldrich). Single-cell suspensions were stained with a combination of the following antibodies: allophycocyanine-conjugated anti-F4/80 (eBioscience, BM8), allophycocyanine-cyanine 7-conjugated anti-CD11b (BioLegend, M1/70), phycoerythrin-cyanine 7-conjugated anti-CD11c (BD PharMingen, HL3), and eFluor 450-conjugated CD45 (eBioscince, 30-F11).

Dead cells were stained with via-probe (Becton Dickinson). Stained samples were analyzed with FACSAria II (Becton Dickinson and Company) and FlowJo software (TreeStar).

RNA isolation and integrity. Venus-positive and -negative cells from three pooled lungs were collected in TRIzol Reagent (Invitrogen). Total RNA was extracted by isopropanol precipitation with glycogen as a carrier. Isolated total RNA integrity was assessed by determining UV 260/280 absorbance ratios and by examining 28S/18S ribosomal RNA bands with an Agilent 2100 bioanalyzer (Agilent Technologies) according to the manufacturer's instructions.

Microarray analysis. Forty nanograms of total RNAs was amplified by using the Arcturus® Riboamp® Plus RNA Amplification Kit (Life technologies). Cy3-labeled complementary RNA probe synthesis was initiated with 100 ng of total RNA by using the Agilent Low Input Quick Amp Labeling kit, one color (Agilent Technologies) according to the manufacturer's instructions. The Agilent SurePrint G3 Gene Mouse GE 8 × 60 K microarray was also used. Slides were scanned with an Agilent's High-Resolution Microarray Scanner, and image data were processed by using Agilent Feature Extraction software ver. 10.7.3.1. All data were subsequently uploaded into GeneSpring GX ver 12.5 for data analysis. For the data analysis, each gene expression array data set was normalized to the *in silico* pool for samples from mice inoculated with PBS. Statistically significant differences in gene expression between the Venus-positive cells and -negative cells were determined by using one-way analysis of variance (ANOVA) followed by the Turkey HSD post-hoc test ($P < 0.05$) and the Benjamin-Hochberg false discovery rate

16

correction. Differentially expressed genes were further filtered to include genes whose expression changed 2.0-fold relatively to the level in the PBS group. Genes that passed the statistical analysis were further assigned to a gene ontology (GO) grouping.

Results

Establishment of a mouse-adapted NS1-Venus PR8 virus. Although I successfully rescued NS1-Venus PR8 WT virus by reverse genetics, this virus was avirulent in mice (MLD_{50} : $> 10^5$ PFU) and the expression of Venus was very weak in MDCK cells and in the lung sections of mice infected with this virus. To increase the virulence and Venus expression of NS1-Venus PR8 WT virus, the virus was serially passed in mice via intranasal infection with plaque-purified high Venus-expressing clones (see Materials and Methods). After six serial passages, the virulence of the virus appeared to have increased; therefore, I sequenced this mouse-adapted NS1-Venus PR8 WT virus to look for mutations.

The sequence analysis revealed that two amino acid substitutions had occurred after passaging (Table 1). One of the mutations was in PB2 (a glutamine acid-to-asparagine acid substitution at position of 721), and the other was in HA (a threonine-to-alanine substitution at position of 380). To confirm their contribution to pathogenicity in mice, I introduced these mutations into a correspondent polI plasmid, and used reverse genetics to generate NS1-Venus PR8, which possessed the two mutations (referred to as NS1-Venus PR8 MA virus). The pathogenicity of NS1-Venus PR8 MA virus was higher than that of NS1-Venus PR8 WT virus (MLD_{50}: 2.1×10^4 PFU). Furthermore, the Venus signal in the lungs from mice infected with NS1-Venus PR8 MA virus was strong, whereas in the lung infected with NS1-Venus PR8 WT and that infected with PR8, no Venus signal was detected (Fig. 1). NS1-Venus PR8 MA, therefore, showed promise as a useful reporter virus, and I continued to analyze this virus in detail.

Protein	amino acid position	amino acid encoded	
		PR8	NS1-Venus PR8 MA
PB2	712	E	D
HA	380	T	A

Table 1. Amino acid substitutions in NS1-Venus PR8 MA virus.

NS1-Venus PR8 MA **PR8**

NS1-Venus PR8 WT **PBS**

CD11b Venus Hoechst33342
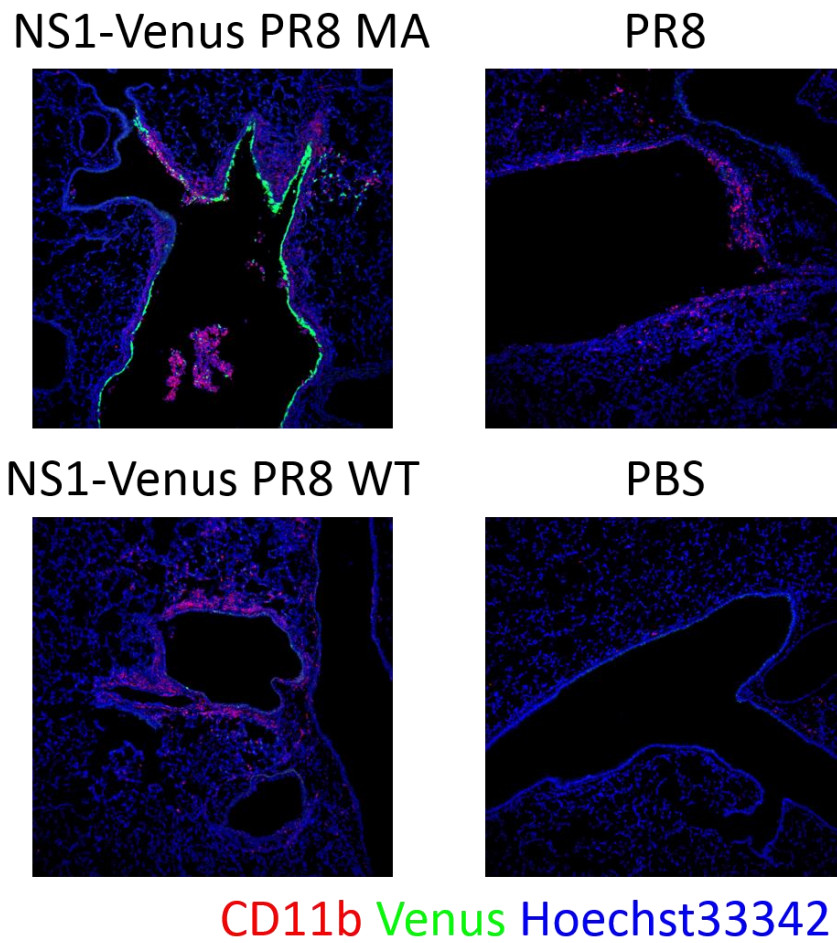
Fig. 1. High Venus expression of NS1-Venus PR8 MA virus in mouse lung.

Venus expression in lung from mice infected with each virus was observed. Three days after infection, lungs were collected and frozen sections were prepared. An anti-CD11b antibody was used to detect macrophages and monocytes, which accumulated at inflamed sites. Hoechst33342 was used to stain cell nuclei. Samples were observed by using a confocal microscope. Representative data are shown.

Comparison of mutant virus replication in MDCK cells. To compare the growth of these viruses in a cell line, I generated two single-gene reassortants that possessed the PB2 or HA gene of NS1-Venus PR8 MA virus and the remaining genes from NS-Venus PR8 WT virus for use in experiments with the NS1-Venus PR8 WT and NS1-Venus PR8 MA viruses. MDCK cells were infected with these viruses at an MOI of 0.001 and viral titers in supernatants were determined every 12 h by means of a plaque assay (Fig. 2). Although NS1-Venus PR8 WT virus grew to $10^{6.5}$ PFU/ml, NS1-Venus PR8 MA virus grew to more than 10^8 PFU/ml, comparable to wild-type PR8 virus. While the viral titers of NS1-Venus PR8 PB2 virus and NS1-Venus PR8 HA virus reached approximately $10^{7.5}$ PFU/ml, these were lower than that of NS1-Venus PR8 MA virus. Therefore, the growth capability of NS1-Venus PR8 MA virus was remarkably improved in MDCK cells, and the mutations in the PB2 and HA genes acted in an additive manner.

Comparison of the pathogenicity and replication in mice of the mutant viruses. Next, to assess their pathogenicities, I infected C57BL/6 mice with 10^5, 10^4 or 10^3 PFU of these viruses and monitored their body weights and survival (Fig. 3). The body weights of the mice infected with 10^5 PFU of these viruses dramatically decreased and 1 out of 4 mice infected with NS1-Venus PR8 WT virus and all of the mice infected with NS1-Venus PR8 PB2 and NS1-Venus PR8 MA virus had to be euthanized during the observation period. In addition, mice infected with 10^4 PFU of NS1-Venus PR8 PB2 and NS1-Venus PR8 MA virus showed pronounced body weight loss, and 1 out of 4 mice infected with NS1-Venus MA virus and 2 out of 4 mice infected with NS1-Venus PR8 PB2 virus succumbed to their infection. On the other hand, although the body weights of the mice infected with 10^4 PFU of NS1-Venus PR8 HA and NS1-Venus PR8 WT virus
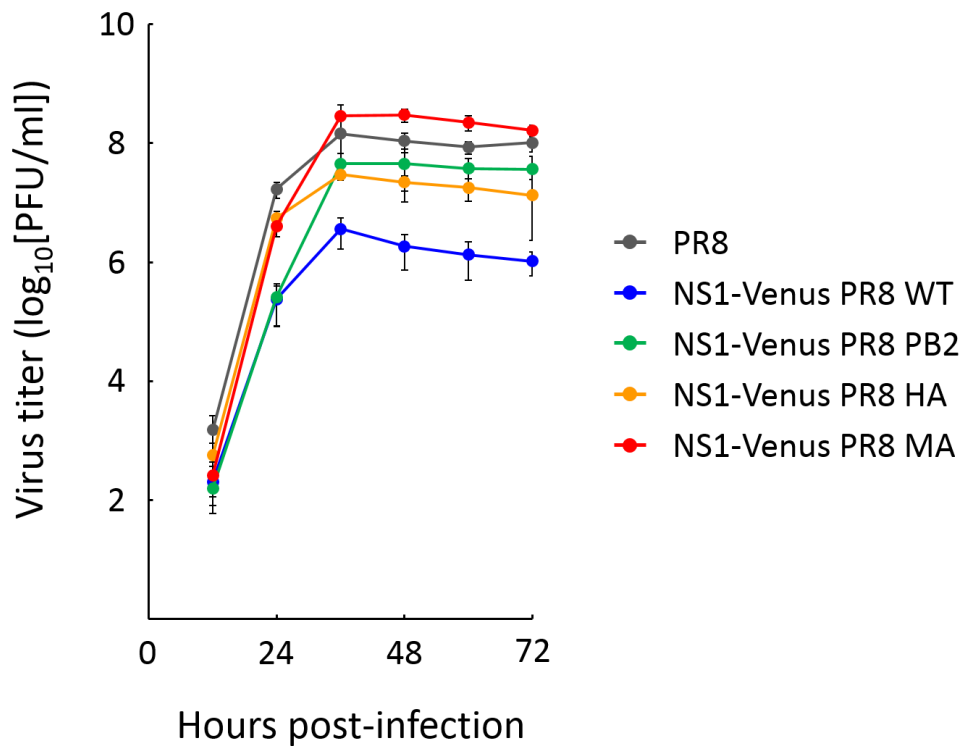
Fig. 2. Comparison of the growth capabilities of mutant viruses in MDCK cells.

MDCK cells were infected at a MOI of 0.001 with PR8, NS1-Venus PR8 WT, NS1-Venus PR8 MA, and mutant NS1-Venus PR8 viruses that possess amino acid substitutions found in NS1-Venus PR8 MA virus. Virus titers were determined every 12 h by means of plaque assays. Results are expressed as the mean titer (log₁₀ [PFU/ml]) ± standard deviation.
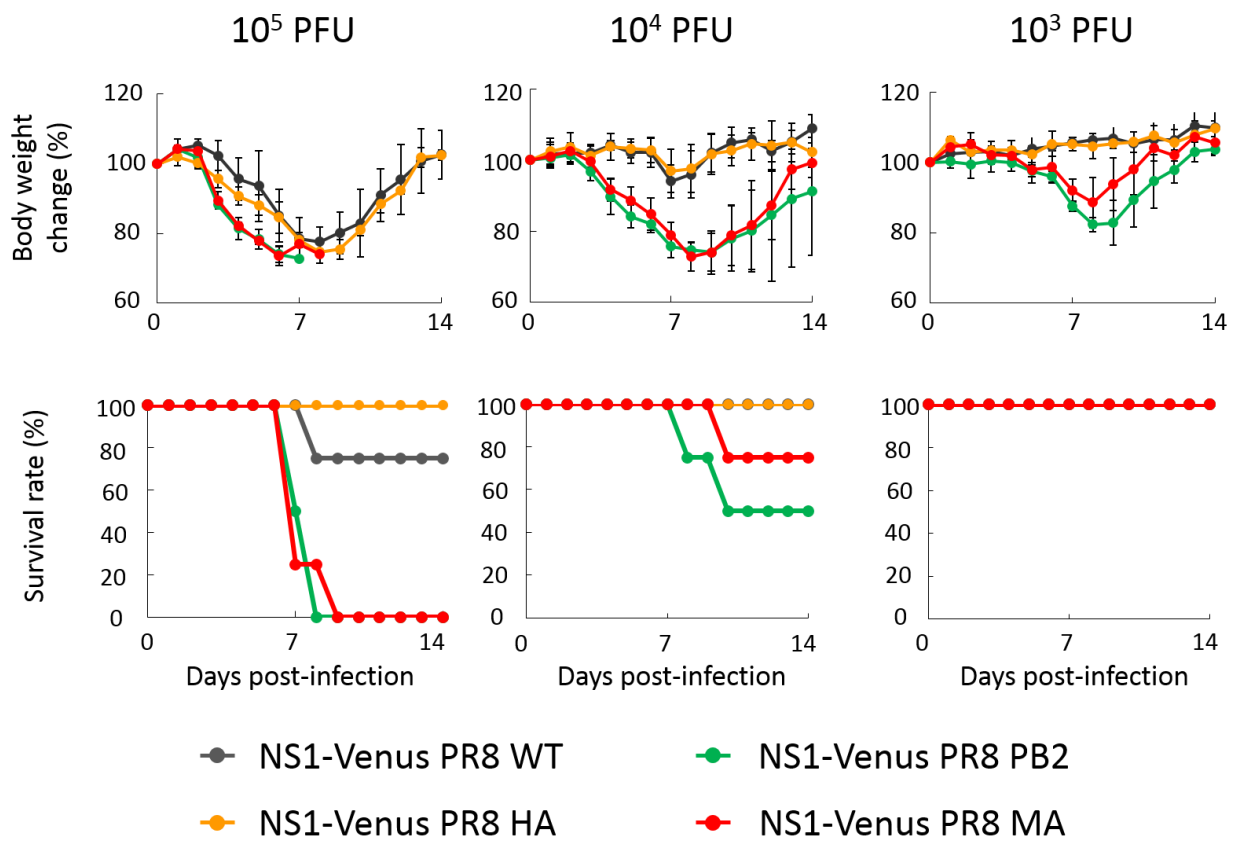
Fig. 3. Body weight changes and survival rates for mice infected with viruses carrying Venus.

Four mice per group were intranasally infected with 10^3, 10^4 and 10^5 PFU of each NS1-Venus PR8 virus. Body weights were measured and survival rates were monitored for 14 days after infection.

decreased slightly, all of the mice survived. In the case of infection with 10^3 PFU, while the body weights of the mice infected with NS1-Venus PR8 PB2 and NS1-Venus PR8 MA decreased slightly, all of these mice also survived. Mice infected with 10^3 PFU of NS1-Venus PR8 WT and NS1-Venus PR8 HA showed little body weight loss, and all of the mice survived. I also determined the viral titers of these viruses in mouse lung (Fig. 4). Mice were infected with 10^3 PFU of the viruses and lungs were collected on days 3, 5, and 7 after infection. The maximum virus lung titer from mice infected with NS1-Venus PR8 PB2 virus was $> 10^6$ PFU/g, which was similar to that from mice infected with NS1-Venus PR8 MA virus. In contrast, virus titers in lungs from mice infected with NS1-Venus PR8 WT and NS1-Venus PR8 HA virus were significantly lower than those in lungs from mice infected with NS1-Venus PR8 PB2 and NS1-Venus PR8 MA virus at all time points. Finally, viruses were not detected in lungs from mice infected with NS1-Venus PR8 WT at 7 days after infection. Taken together, these results demonstrate that only the PB2 mutation affected the pathogenicity and replication of NS1-Venus PR8 MA virus in mice.

The stability of Venus expression by NS1-Venus PR8 MA virus during replication *in vitro* and *in vivo*. In the Manicassamy study (Manicassamy et al., 2010), the proportion of GFP-negative virus increased over time. This is one of the obstacle to utilizing this virus for live imaging studies. I, therefore, assessed the stability of the Venus expression by NS1-Venus PR8 MA virus during replication in MDCK cells (Fig. 5A). I found that more than 90% of plaques were Venus-positive even 72 h after infection. I also checked the positive rate of Venus expression during repeated passages of the virus in cell culture (Fig. 5B). Approximately 90% of plaques expressed Venus even after 5 passages,
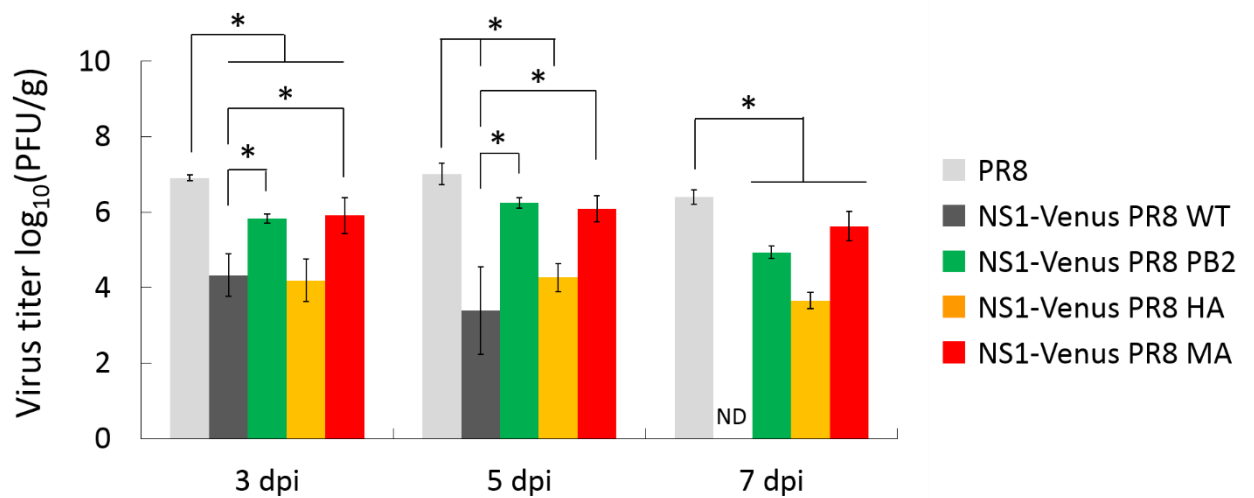
Fig. 4. Virus titers in mouse lung.

Nine mice per group were intranasally infected with 10^3 PFU of PR8 or the respective NS1-Venus PR8 virus. Three mice per group were euthanized on days 3, 5, and 7 after infection and their lungs collected to determine virus titers. Virus titers were determined by means of plaque assays. Results are expressed as the mean of the titer (log_{10} PFU/g) ± standard deviation. Statistical significance was calculated by using the Tukey-Kramer method. Asterisks indicate significant differences from titers from mice infected with PR8 or NS1-Venus WT virus ($P < 0.05$). ND: Not detected (detection limit, 5 PFU/lung)
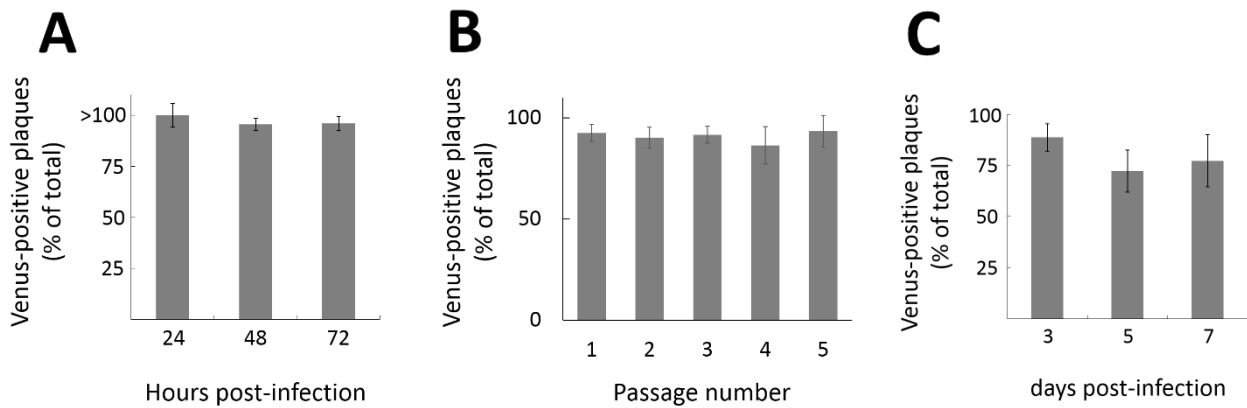
Fig. 5. The stability of Venus expression by NS1-Venus PR8 MA virus *in vitro* and *in vivo*. The positive rate of Venus expression was examined in MDCK cells (A, B) and in mouse lung (C). (A) MDCK cells were infected with NS1-Venus PR8 MA virus at an MOI of 0.001, and supernatants were collected every 24 h. The positive rate of Venus expression was estimated by dividing the number of plaques that expressed Venus by the total number of plaques. (B) NS1-Venus PR8 MA virus was serially passaged in MDCK cells five times and the positive rates of Venus expression were estimated. (C) Nine mice were infected with 10^3 PFU of NS1-Venus PR8 MA virus. Three mice were euthanized at each time point and plaque assays were performed using lung homogenates. The positive rates of Venus expression were estimated as described above.

suggesting that Venus expression by NS1-Venus PR8 MA virus was stable in cell culture. Finally, I confirmed that Venus expression was stable during virus replication *in vivo* (Fig. 5C). I performed a plaque assay using lung homogenates and estimated the positive rate of Venus expression essentially as described above. Although the percentage of Venus-positive plaques was more than 85% at 3 days after infection, that of Venus-positive plaques was approximately 75% at 7 days after infection. Taken together, these results indicate that Venus expression by NS1-Venus PR8 MA virus is stable during replication *in vitro*, and the percentage of Venus-positive plaques in mouse lung was similar to that reported previously (Manicassamy et al., 2010).

The PB2-E712D substitution is responsible for high Venus expression. The Venus expression level of NS1-Venus PR8 MA virus was substantially higher than that of NS1-Venus PR8 WT virus. Since PB2 is one of the subunit of the influenza virus polymerase, I hypothesized that the PB2-E712D substitution was important for the augmentation of Venus expression. To compare the Venus protein expression, I performed western blots of the viral protein and Venus in infected cells (Fig. 6A). Twelve hours post-infection, although the amount of M1 protein was similar for all of the viruses, the amount of Venus protein was higher in cells infected with NS1-Venus PR8 PB2 and NS1-Venus PR8 MA virus compared with the other two viruses that possessed the parental PB2 gene. I also observed Venus expression in infected cells by using a confocal laser microscope (Fig. 6B). As expected, the Venus signals in the cells infected with NS1-Venus PR8 PB2 and NS1-Venus PR8 MA virus were stronger than in the cells infected with the two viruses that possessed parental PB2 gene. Taken together, these results demonstrate that the PB2-E712D substitution was responsible for the high Venus expression.
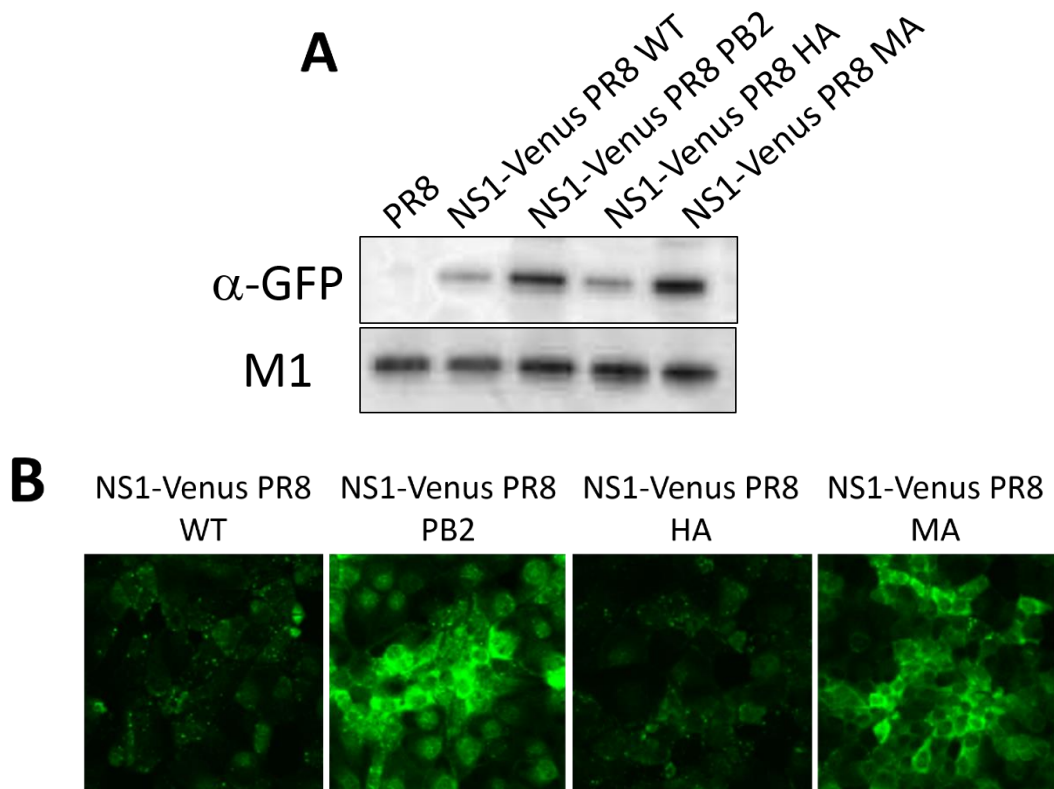
Fig. 6. Comparison of Venus expression in cells infected with each NS1-Venus PR8 virus.

(A) Venus protein expression in cells infected with each NS1-Venus PR8 virus was detected by means of western blotting. MDCK cells were infected with each virus at an MOI of 1. Twelve hours after infection, virus-infected cells were lysed and western blotting was performed. An anti-GFP antibody was used to detect Venus protein, and M1 protein was detected as a control. The bands appeared at approximately 27 kDa were shown in M1 panel. Representative results of two independent experiments are shown. (B) Observation of Venus expression by use of confocal microscopy. MDCK cells were infected with each virus at an MOI of 1. Twelve hours after infection, cells were fixed, and Venus expression was observed. Representative results of two independent experiments are shown.

The HA-T380A substitution raises the threshold for membrane fusion. The major functions of the HA protein are receptor binding and membrane fusion. Because the HA-T380A substitution was located on the α-helix of the HA2 subunit, I anticipated it would have an effect on the membrane-fusion activity of HA. To test this possibility, I performed a polykaryon formation assay (Fig. 7). The wild-type HA had a threshold for membrane fusion of pH 5.5, whereas the threshold for HA-T380A increased to pH 5.8. These data indicate that the HA-T380A mutation allows the mutant HA to initiate membrane fusion at a higher pH than occurs with parental HA.

Time-course observation of virus propagation in whole mouse lung. NS1-Venus PR8 MA virus allows us to observe virus-infected cells without immunostaining, because the Venus expression by this virus is sufficiently high to permit the visualization of infected cells with a microscope. I attempted to observe how influenza virus propagates in the lung by using transparent lungs treated with SCALEVIEW A2, a recently developed reagent that make samples optically transparent without decreasing fluorescence intensity (Fig. 8). Mice were intranasally infected with 10^5 PFU of PR8, NS1-Venus PR8 WT, and NS1-Venus PR8 MA virus, and lungs were collected on days 1, 3, and 5 after infection. After treatment with SCALEVIEW A2, I observed the samples by using a stereo fluorescence microscope. At first, I tried to directly observe the transparent lobe of the lung (Fig. 8, upper panel, "intact"), but the Venus signals were ambiguous because of insufficient transparency. Therefore, I dissected the transparent samples in the direction of the long axis to expose the bronchi (Fig. 8, lower panel, "cut"). I was unable to observe Venus expression in the transparent samples from mice infected with NS1-Venus PR8 WT virus at any time point (Fig. 8G, H. Samples collected at 3 days
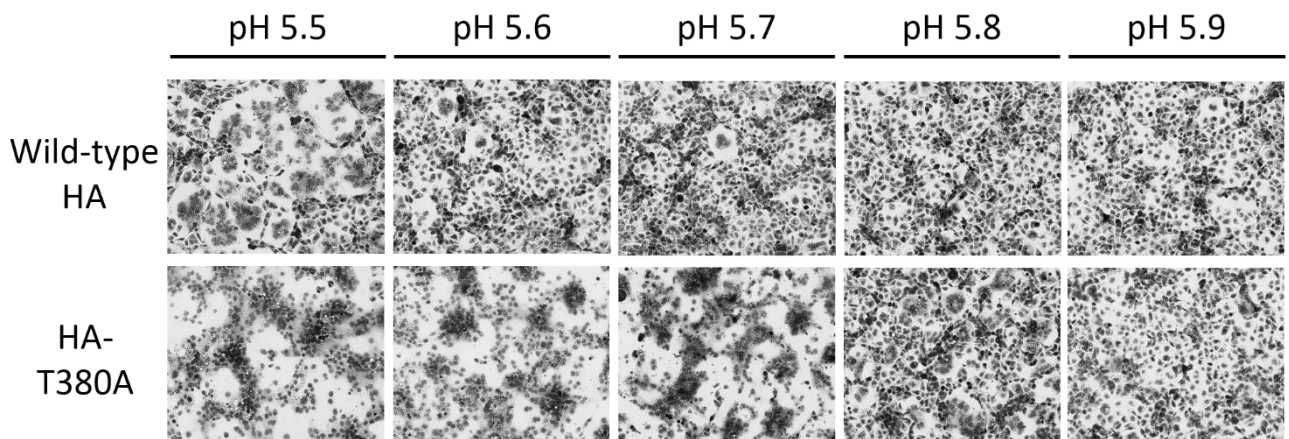
Fig. 7. Polykaryon formation by HEK293 cells infected with wild-type PR8 or PR8 that possesses the HA-T380A mutation after exposure to low pH buffer.

The threshold for membrane fusion was examined at a pH range of 5.5–5.9. HEK293 cells were infected with PR8 or PR8 that possesses the HA-T380A substitution. Eighteen hours after infection, HA on the cell surface was digested with TPCK-trypsin, and exposure to the indicated pH buffer. After fixation with methanol, the cells were stained with Giemsa's solution. Representative pictures are shown.
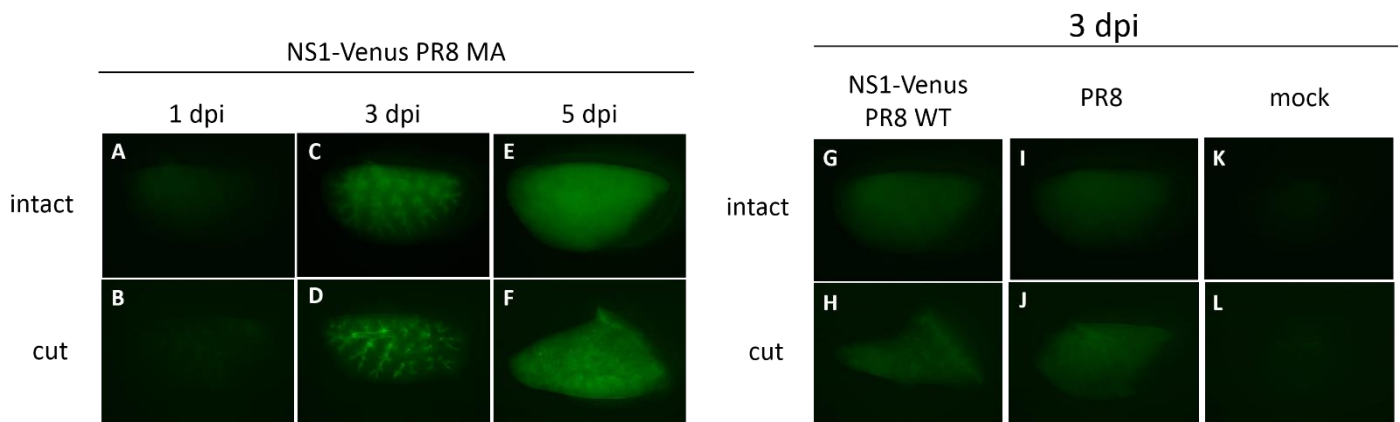
Fig. 8. Time-course observation of Venus-expressing cells in transparent lungs.

Venus-expressing cells in whole lung lobe were observed. Three mice per group were intranasally infected with NS1-Venus PR8 MA (A–F), NS1-Venus PR8 WT (G, H) or PR8 (I, J) virus and lungs were collected on the indicated days. Mock-treated lungs served as a negative control (K, L). To image Venus-expressing cells deeper, lung samples were treated with SCALEVIEW A2, which make samples transparent, and were separated into each lobe and observed by using a stereo fluorescence microscope. After imaging the whole lung lobe (intact), samples were dissected to exposure the bronchi (cut). Samples from mice infected with PR8 or NS1-Venus PR8 WT virus were prepared on day 3 post-infection to compare with NS1-Venus PR8 MA virus-infected lungs in which the Venus signal was the brightest during infection. Representative images are shown.

post-infection are shown). In the case of NS1-Venus PR8 MA virus-infected lungs, although Venus signals were not observed at 1 day post-infection (Fig. 8A, B), Venus expression was clearly observed in a large portion of the epithelial cells of the bronchi at 3 days post-infection (Fig. 8C, D). Venus expression was also occasionally observed in alveolar epithelial cells around the bronchus. At 5 days post-infection, most of the Venus-positive cells found in the bronchial epithelium had disappeared and the number of Venus-positive cells in the bronchiole and alveoli had increased (Fig. 8E, F). On the basis of these observations, it may be that the Venus-positive cells found in the bronchi at 3 days post-infection died and the influenza virus spread from the bronchi to the bronchioles and alveoli over time. I did not observe any obvious Venus signal in the transparent lungs from the mice inoculated with PR8 or PBS (Fig. 8I–L). These results demonstrate that NS1-Venus PR8 MA virus and transparent reagent SCALEVIEW A2 permit the visualization of the dynamics of influenza virus infection in whole lung lobes.

Identification of the target cells of NS1-Venus PR8 MA virus in mouse lung.
My observation of transparent lung infected with NS1-Venus PR8 MA virus revealed that influenza virus first infected the bronchial epithelium and subsequently invaded the alveoli over time. Next, to identify the target cells of NS1-Venus PR8 MA virus, I performed an immunofluorescence assay of frozen sections by using several antibodies specific for lung cells (Fig. 9). The epithelial cells of the bronchi and bronchioles include Clara cells, ciliated cells, goblet cells, and a small number of neuroendocrine cells, whereas alveoli comprise type I and type II alveolar epithelial cells. Of these cell types, I focused on Clara cells and type II alveolar epithelial cells because Clara cells constitute the bulk of the lumen of bronchi and bronchioles (Rawlins et al., 2006), and type II

alveolar epithelial cells have previously been reported to be a target of influenza virus (Baskin et al., 2009). At 3 days post-infection, a large proportion of the bronchiole cells were Venus-positive and almost all of these cells were CC10-positive (Fig. 9A). In addition, cuboidal Venus signals in the alveolar regions were merged with SP-C positive cells (Fig. 9B, white arrowheads). Although rare, Venus-positive type I alveolar epithelial cells were observed at 5 days post-infection (Fig. 9B, white arrow). However, I never detected Venus expression in neuroendocrine cells (data not shown).

I also performed flow cytometry to determine whether alveolar macrophages and monocytes were infected with NS1-Venus PR8 MA virus, because these immune cells are present in lung and function as the first line of defense against inhaled microbes and particulates. I distinguished between alveolar macrophages and monocytes on the basis of the CD11b expression level in the F4/80$^+$ population (Fig. 10A). Mice were infected with 10^5 PFU of PR8 or NS1-Venus PR8 MA virus and the total number of these cells were compared. After influenza virus infection, although the number of alveolar macrophages was rarely different from that of the control group, the number of monocyte dramatically increased because monocytes infiltrated sites of infection from blood vessels (Fig. 10B, C). As to the proportion of Venus-positive cells, 3.16% ± 0.59% of the alveolar macrophages were Venus-positive cells and 1.55% ± 0.07% of the monocytes were Venus-positive at 3 days post-infection (Fig. 10D, E). Further, the number of Venus-positive cells decreased slightly between 3 days and 5 days after NS1-Venus PR8 MA virus infection. For the PR8 infection, the number of Venus-positive cells was comparable to that in mock-treated mice. Taken together, these results demonstrate that the Clara cells in the bronchus and bronchiolus, type II alveolar epithelial cells, monocytes, and alveolar macrophages in the alveolar regions of the lung are target cells of influenza virus.
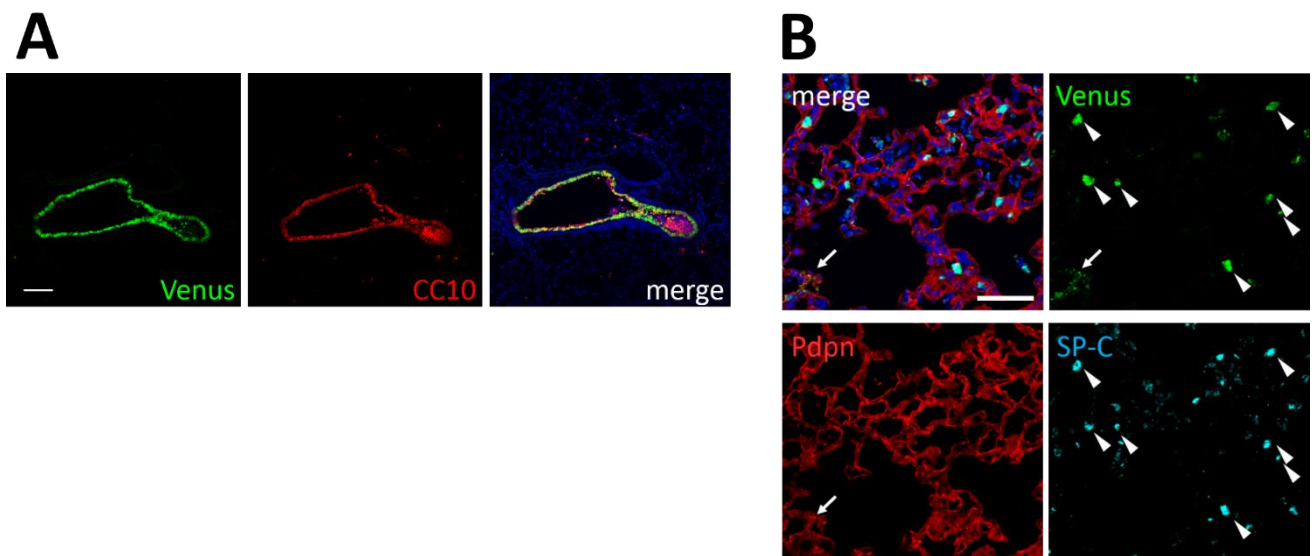
Fig. 9. Analysis of Venus expression in CC10+ cells and SP-C+ cells in lungs.

Lung sections from mice infected with NS1-Venus PR8 MA virus were stained with several antibodies specific for the epithelial cells in the lung. Mice were infected with 10^4 PFU of NS1-Venus PR8 MA virus and lungs were collected at 3 and 5 days post-infection. (A) Lung section of mice infected with NS1-Venus PR8 MA virus were prepared at 3 days post-infection and stained with an anti-CC10 polyclonal antibody (red). Scale bar: 100 μm. (B) Lung section of mice infected with NS1-Venus PR8 MA virus were prepared at 5 days post-infection and stained with an anti-SP-C polyclonal antibody (cyan) and an anti-podoplanin (Pdpn) polyclonal antibody (red). Venus-positive cells in the alveolar region comprised SP-C-positive cells (white arrowhead) and podoplanin-positive cells (white arrow). Scale bar: 50 μm.
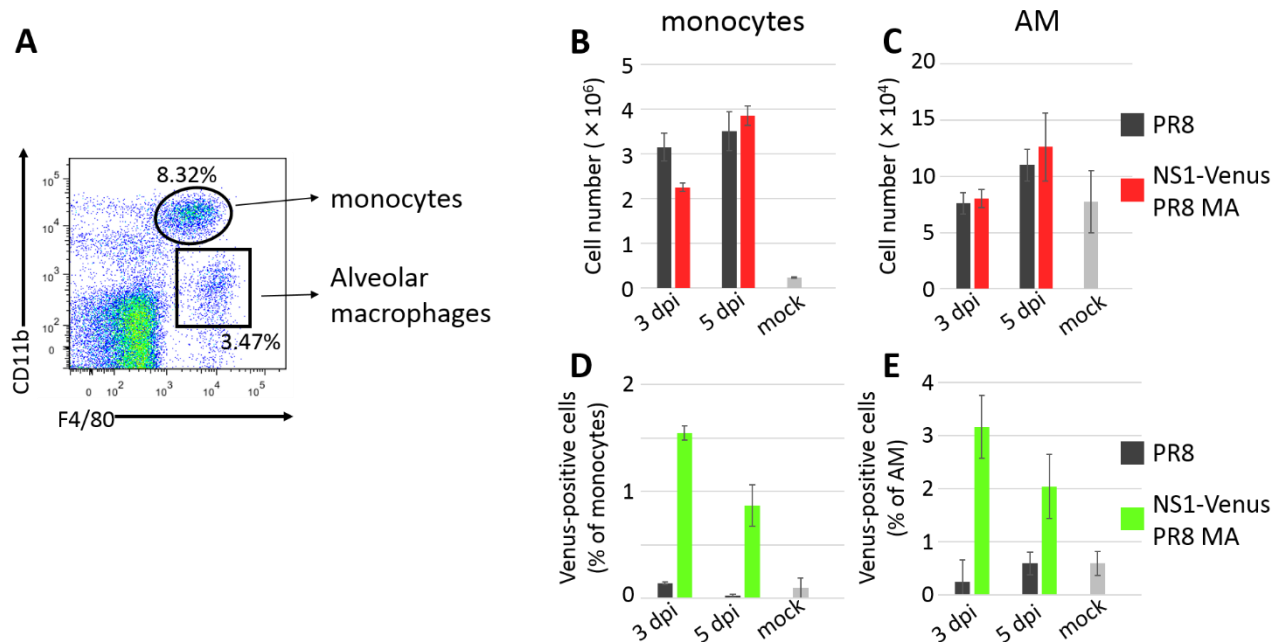
Fig. 10. Flow cytometric analysis of Venus-positive cells in specific cell types of the lung.

Venus-positive cells in the indicated cell types were analyzed by using flow cytometry. Mice were infected with 10^5 PFU of PR8 or NS1-Venus PR8 MA virus and lungs were collected at 3 and 5 days post-infection. Single cell suspensions were stained with antibodies. (A) Representative dot plot for CD45$^+$ live cells from the lung of mice inoculated with PBS are shown. (B, C) Total numbers of each specific cell species at the indicated time points are shown. Results are expressed as the mean cell numbers per lung $\pm$ standard deviation. CD45$^+$ and via-probe$^-$ cells were analyzed for monocytes and alveolar macrophages. (D, E) The numbers of Venus-positive cells in cells defined in A and B at the indicated time points are shown. Results are expressed as the mean cell numbers $\pm$ standard deviation. AM: alveolar macrophage.

Differential gene expressions between Venus-positive and -negative cells in the F4/80$^+$ cell population. Because alveolar macrophages and monocytes act as the first line of defense against inhaled microbes, it is possible that infection of these cells with influenza virus might influence their ability to prevent the spread of infection. To assess this, I attempted to compare the gene expression profiles between the Venus-positive and -negative cells among the alveolar macrophage and monocyte populations by means of microarray analysis. Because the number of Venus-positive alveolar macrophages and monocytes that could be collected from one mouse by using flow cytometry was too small to perform a microarray analysis, these cells were analyzed together as F4/80$^+$ cells and pooled from three mice. Live mononuclear cells were gated as CD45$^+$ and via-probe$^-$ cells. As shown in Fig. 10A, the cells were confirmed as alveolar macrophages and monocytes on the basis of CD11b expression levels in the F4/80$^+$ population. Venus-positive and -negative F4/80 cells were sorted from a fraction of the live mononuclear cells by FACSAria II. Since CD11c^{high} alveolar macrophages possess high autofluorescence, the possibility existed for overlap with the Venus signal. Therefore, CD11c^{high} alveolar macrophages with intermediate expression of Venus were excluded from the Venus-positive fraction (Fig. 11A). From my confocal microscopic observation of the sorted cells, I confirmed that these cells could be collected properly based on Venus expression (Fig. 11B). In addition, given that Venus expression was observable throughout the cell, these cells would have been infected with virus, but did not engulf the infected cells. The microarray analysis revealed thousands of genes whose expression statistically changed at least 2.0-fold relative to the level of F4/80$^+$ cells from mice inoculated with PBS (data not shown). Among these genes, 633 genes whose expression statistically differed by at least 4.0-fold between Venus-positive and -negative F4/80$^+$ cells were identified (Fig.
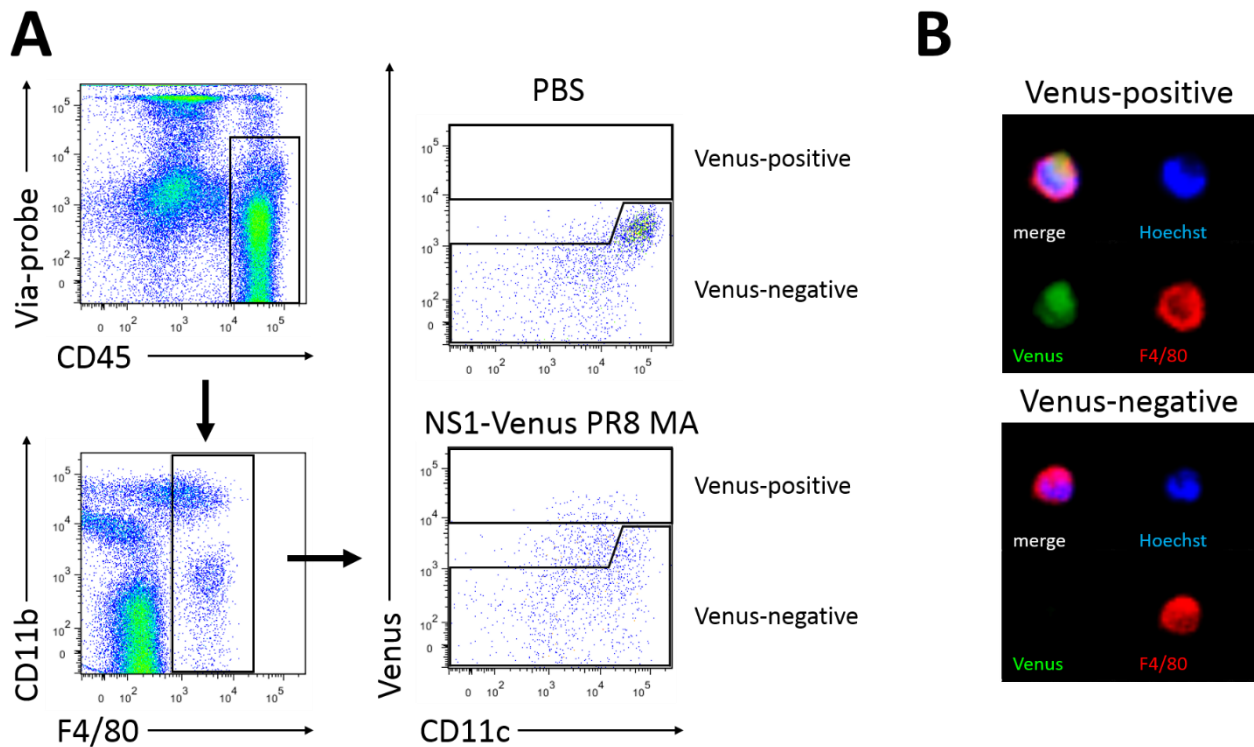
Fig. 11. Sorting strategy to collect Venus-positive and Venus-negative cells in the F4/80[+] population.

Mice were infected with 10^5 PFU of NS1-Venus PR8 MA virus and lungs were collected at 3 days post-infection. Single cell suspensions were stained with a set of antibodies. Lungs from mice inoculated with PBS were similarly stained to confirm the autofluorescence of alveolar macrophages. (A) Representative dot plots showing the gating strategy to collect Venus-positive and -negative cells in a population of CD45^{+}, via-probe^{-} F4/80^{+} cells. The Venus-positive gate was shown not to include alveolar macrophages. (B) Venus-positive and -negative cells collected from the lungs of mice infected with NS1-Venus PR8 MA virus were observed by using an immunofluorescence assay.

12A). Gene Ontology analysis revealed that these genes were involved in extracellular activity (Fig. 12B). I focused on the genes annotated in "cytokine activity"; a total of 24 genes had changed expression levels, including several cytokines, such as type I interferon (IFN), and chemokines (Fig. 12C). All of these genes except for the genes for interleukin (IL)-4 and Cxcl13 [chemokine (C-X-C motif) ligand 13] were up-regulated in Venus-positive cells relative to Venus-negative cells. Moreover, when I focused on the genes annotated in "response to wounding", most genes including those for collagen type 1α1 (Col1a1), collagen type 3α1 (Col3a1), collagen type 5α1 (Col5a1), hyaluronoglucosamidase 1 (Hyal1), and fibrinogen γ chain (Fgg) were up-regulated in Venus-positive F4/80$^+$ cells (Fig. 12D). Taken together, these results demonstrate that a small number of cells relative to the total number of F4/80$^+$ cells was infected with influenza virus and that the gene expression levels of several cytokines and chemokines were enhanced in the virus-infected cells at the site of infection. Furthermore, F4/80$^+$ cells infected with NS1-Venus PR8 MA virus enhanced the expression of genes involved in the response to wounding which would be caused by infection and inflammation.
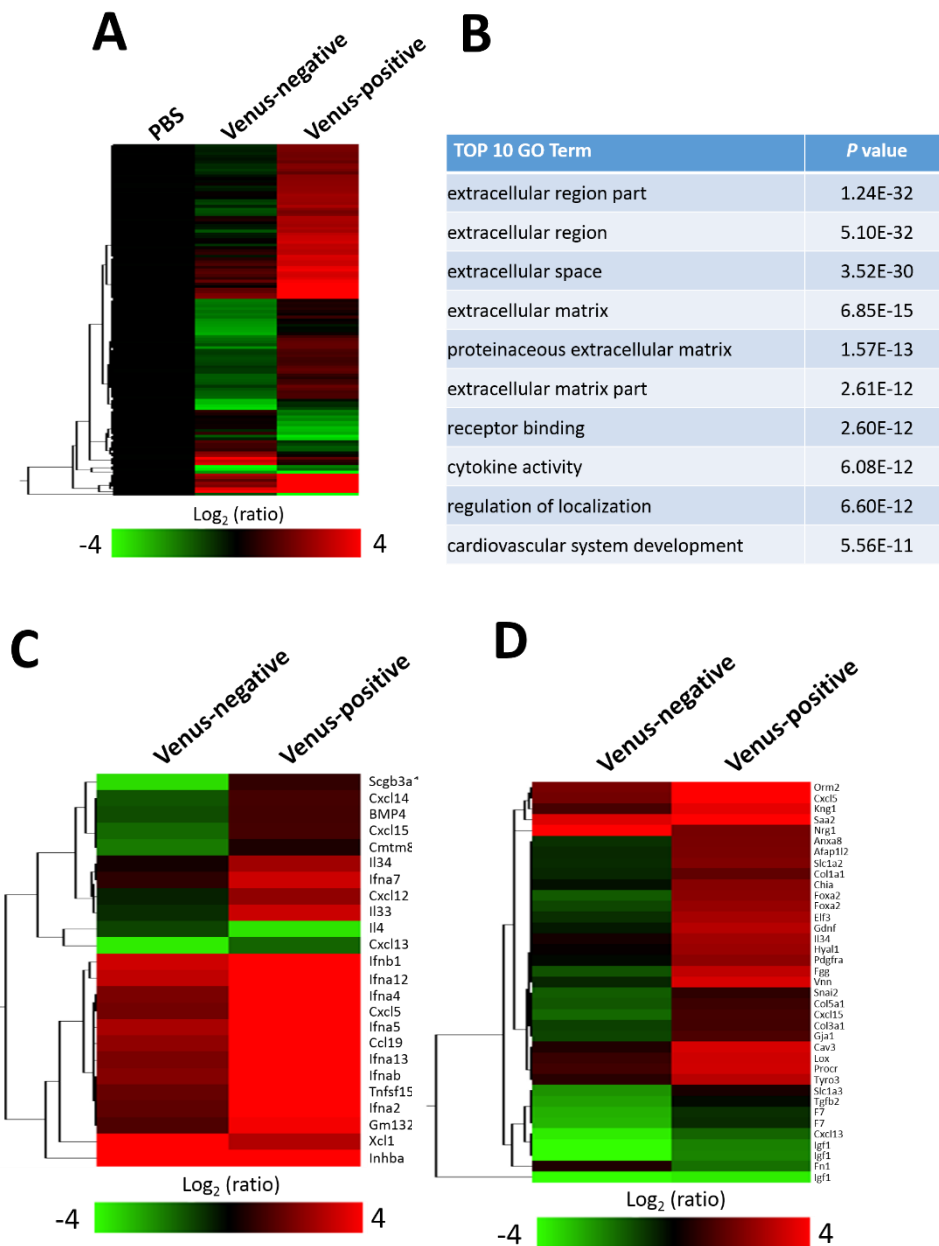
Fig. 12. Genes differentially expressed between Venus-positive and -negative F4/80$^+$ cells.

Mice were infected with 10^5 PFU of NS1-Venus PR8 MA virus and lungs were collected at 3 days post-infection. Single cell suspensions were stained in the same manner as described in Fig. 10. Venus-positive and -negative cells were separately harvested by using FACSAria II and subjected to microarray analysis. F4/80$^+$ cells

isolated from the lungs of mice inoculated with PBS were used as a control. (A) A total of 633 genes were selected by student's T test ($P < 0.05$) and by filtering the genes whose expression changed at least 4.0-fold between the Venus-positive and- negative groups from the genes whose expression changed at least 2.0-fold from the level of the PBS group. (B) These selected genes were functionally annotated by using Gene Ontology (GO) grouping. Statistical significance were determined by using Fisher's exact test ($P < 0.01$). (C) Hierarchical analysis of genes annotated in "cytokine activity" enriched by genes that were significantly differentially expressed between Venus-positive and- negative F4/80^{+} cells. (D) Hierarchical analysis of genes annotated in "response to wounding" enriched by genes that were significantly differentially expressed between Venus-positive and -negative F4/80^{+} cells.

Discussion

A reporter influenza virus is useful to analyze the dynamics of influenza virus infection. Although NS1-GFP virus could replicate *in vitro* and *in vivo* and exhibited pathogenicity in BALB/c mice, GFP expression was not strong and GFP-negative viruses were detected over time during replication. Indeed, low Venus expression was also confirmed in our NS1-Venus PR8 WT virus. After six passages in mice and MDCK cells, the Venus expression and stability of our NS1-Venus PR8 MA virus was substantially improved, although Venus-negative viruses emerged as with previous study during replication in mouse lung. While the pathogenicity of NS1-Venus PR8 MA virus was attenuated to some extent, its replication in mouse lung and in cell culture was enhanced. Therefore, I believe that this reporter virus will be useful in a variety of influenza-related fields given its high Venus expression and replication ability.

I identified two amino acid substitutions in the PB2 and HA genes, respectively, of NS1-Venus PR8 MA virus. Given that the body weight loss of mice infected with NS1-Venus PR8 PB2 virus was almost identical to that of mice infected with NS1-Venus PR8 MA virus, it is likely that the PB2-E712D substitution was responsible for the pathogenicity of NS1-Venus PR8 PB2 virus. Indeed, the virus titer in the lungs from mice infected with NS1-venus PR8 PB2 virus was comparable to that in the lungs from mice infected with NS1-venus PR8 MA virus. In highly pathogenic avian influenza viruses, several amino acid substitutions have been found in PB2 that are involved in the high virulence of these viruses in mammals. For example, a glutamic acid to lysine substitution at position 627 and an aspartic acid to asparagine substitution at position 701 in PB2 are known to influence virulence in mice (Hatta et al., 2001; Li et al., 2005). These mutations

in PB2 change the temperature sensitivity and polymerase activity of the virus (Hatta et al., 2007; Gabriel et al., 2005); however, polymerase activity and pathogenicity are not necessarily correlative (Gabriel et al., 2005). Therefore, the detailed mechanisms remain unclear. There have been no previous reports about the PB2-E712D substitution, supporting the need for further investigation of the effect of this substitution on pathogenicity.

Another amino acid substitution was found in the HA. In MDCK cells, the growth capability of NS1-Venus PR8 HA virus was superior to that of NS1-Venus PR8 WT virus. The polykaryon formation experiment showed that the HA-T380A substitution affected the pH range that induces the conformational change in HA. The elevation of the threshold for membrane fusion could activate the conformational change in HA protein at an earlier stage of endosome maturation during influenza virus entry (Lozach et al., 2011). Further, if a virus can complete membrane fusion and uncoating at an earlier stage of endosome maturation, it is possible for that virus to escape from degradation by lysosomal enzymes. Therefore, viruses that possess the HA-T380A substitution could replicate more efficiently in MDCK cells.

My microarray analysis revealed that the transcriptional levels of several cytokines, including type I IFN, and chemokines were enhanced in Venus-positive F4/80^{+} cells relative to those in Venus-negative F4/80^{+} cells in infected lung. It is likely that innate immune responses were activated upon influenza virus infection in these cells. Further, transcriptional levels of genes involved in the antiviral responses in Venus-negative F4/80^{+} cells were also up-regulated compared with F4/80^{+} cells from PBS-inoculated mice. The activation of these genes was likely elicited by the cytokines secreted in the lung after infection. However, it is possible that Venus-negative cells were

also infected with NS1-Venus PR8 MA virus because antiviral genes begin to be activated before Venus is sufficiently expressed. This is one of the limitation of NS1-Venus PR8 MA virus.

In addition to cytokine and chemokine genes, some genes annotated in "response to wounding" were transcriptionally up-regulated in Venus-positive F4/80$^+$ cells. These virus-infected F4/80$^+$ cells would then be involved in not only antiviral responses but also tissue repair. M2 macrophages (also known as alternatively activated macrophages, AAMs) are thought to contribute to this response. M2 macrophages have an important role in tissue repair and the resolution of inflammation by producing extracellular matrix, such as collagen, and anti-inflammatory mediators, such as IL-10 and resolvin D1 (Sica et al., 2012; Mantovani et al., 2013). Indeed, my microarray data revealed that the expression of arginase-1, which is a marker of M2 macrophages, was markedly up-regulated in Venus-positive F4/80$^+$ cells. A previous study reported that CD11b$^+$ monocytes infiltrate alveoli from blood and are polarized to M2 macrophages by the toll-like receptor (TLR) 2-dependent pathway after priming with *Staphylococcus aureus* (Wang et al., 2013). These cells also contribute to the suppression of inflammatory responses by expressing anti-inflammatory cytokines, such as IL-10 and TGF-β after influenza virus infection (Wang et al., 2013). Therefore, my microarray analysis suggests that the Venus-positive F4/80$^+$ cell population included M2 or M2-like macrophages that were involved in tissue repair and resolution of inflammation, as well classic (M1) macrophages that induced antiviral responses.

In conclusion, given that virus-infected cells in the body are easily detectable by using this virus, I believe that NS1-Venus PR8 MA virus is an important reporter virus that can be utilized for live imaging experiments. By using NS1-Venus PR8 MA virus in

combination with various reporter mice whose immune cells are labeled, we can analyze the spatiotemporal relationship between virus-infected cells and immune cells intravitally. We cannot obtain data on the velocity, distance, and direction of migrating cells by using fixed sample, therefore live imaging experiments will give us new insights into host responses to influenza virus infection.

CHAPTER II

A replication-incompetent virus possessing an uncleavable hemagglutinin as an influenza vaccine.

Abstract

Vaccination is one of the most effective measures to protect against influenza virus infection. Inactivated and live-attenuated influenza vaccines are available; however, their efficacy is suboptimal. To develop a safe and more immunogenic vaccine, I produced a novel replication-incompetent influenza virus that possesses uncleavable hemagglutinin (HA) and tested its vaccine potential. The uncleavable HA was engineered by substituting the arginine at the C-terminus of HA1 with threonine, which prevents cleavage of HA into its HA1 and HA2 subunits, preventing fusion between the host and viral membranes. Although this fusion-deficient HA influenza virus that possesses uncleavable HA (uncleavable HA virus) could undergo multiple cycles of replication in only wild-type HA-expressing cells, it could infect normal cells and express viral proteins in infected cells, but could not generate infectious virus from infected cells due to the uncleavable HA. When C57BL/6 mice were intranasally immunized with the uncleavable HA virus, influenza-specific IgG and IgA antibodies were detected in nasal wash and bronchoalveolar lavage samples and in serum. In addition, influenza-specific CD8$^+$ T cells accumulated in the lungs of these mice. Moreover, mice immunized with the uncleavable HA virus were protected against a challenge of lethal doses of influenza virus, unlike mice immunized with a formalin-inactivated virus. These findings demonstrate that this fusion-deficient virus, which possesses uncleavable HA, is a suitable influenza vaccine candidate.

Introduction

Influenza viruses cause acute respiratory disease and are responsible for epidemics and occasional pandemics as exemplified in 2009 (Dawood et al., 2009; Neumann et al., 2009). Although medical treatment options are well developed, influenza continues to be a great burden on public health and economies worldwide.

Currently, inactivated and live-attenuated vaccines are available. While inactivated vaccines are safe and induce virus-specific immunoglobulin G (IgG) in sera because of intramuscular administration, live-attenuated vaccines, which bear introduced mutations that are responsible for temperature sensitivity and viral attenuation (Maassab et al., 1968; Chen et al., 2006; Hoffmann et al., 2005; Jin et al., 2003; Jin et al., 2004), are more effective because they induce not only virus-specific IgG but also secretory Immunoglobulin A (IgA) at the site of infection following intranasal administration (Cox et al., 2004). In addition to inducing antibodies, live-attenuated vaccines elicit the virus-specific cytotoxic T lymphocytes (CTLs). CTLs specifically lyse infected cells and prevent viral spread. CTLs are also known to have cross-reactivity between different subtypes of influenza A virus. Thus, the induction of CTLs has attracted attention in vaccine development (Rimmelzwaan et al., 2007). Nevertheless adverse effects, such as runny nose, due to replication of the live-attenuated vaccine virus are an issue (Ambrose et al., 2008), and importantly, this live vaccine is not recommended for children under the age of 2, adults aged 50 or over, pregnant women, or immunocompromised patients (Fiore et al., 2010). To overcome current limitations, an ideal influenza vaccine continues to be sought and various strategies have been employed such as virus-like particles (VLPs) (Lambert et al., 2010).

To develop a safe and more effective vaccine that has the merits of inactivated and live-attenuated vaccines, we previously proposed a replication-incompetent virus as a novel influenza vaccine. We reported that NS2-knockout VLPs could efficiently protect mice against lethal doses of influenza virus (Watanabe et al., 2002). However, because of the lack of a cell line that stably expresses NS2 protein, we have to generate VLPs by transfecting plasmids each time.

To overcome this drawback, here I developed a novel replication-incompetent virus that possesses an uncleavable HA (uncleavable HA virus) and assessed its immunogenicity and vaccine efficacy in mice.

Materials and methods

Plasmids. To generate the construct encoding the uncleavable HA gene, we used a plasmid containing the HA gene of A/California/04/09 (CA04) as a template for PCR and primers containing nucleotide replacements at positions 1031 and 1032 of the HA gene, which introduce amino acid substitutions at the cleavage site of HA. This mutated HA gene was cloned into a plasmid under the control of the human polymerase I promoter and the mouse RNA polymerase I terminator (referred as PolI plasmid) as described previously (Neumann et al., 1999). In addition, a plasmid for the expression of wild-type CA04 HA was also constructed by cloning the open reading frame of the CA04 HA gene into an expression plasmid pCAGGS (Niwa et al., 1991).

Cells and viruses. Madin-Darby canine kidney (MDCK) and human embryonic kidney 293T (HEK293T) cells were maintained in minimum essential medium (MEM) containing 5% of newborn calf serum (NCS) and in Dulbecco's modified Eagle medium supplemented with 10% fetal calf serum, respectively. MDCK cells expressing HA from CA04 [HA-MDCK (CA04)] and from A/WSN/33 (WSN) [HA-MDCK (WSN)] were established as follows: for HA-MDCK (CA04) cells, MDCK cells were co-transfected with plasmids for the expression of CA04-HA and puromycin *N*-acetyltransferase, and were cultured in MEM containing 5% NCS and 5 μg/ml puromycin dihydrochloride (Nacalai Tesque). Expression of HA in selected cell clones was confirmed by means of immunostaining with an anti-CA04 HA antibody. For HA-MDCK (WSN), MDCK cells were transfected with plasmids expressing WSN-HA and WSN-neuraminidase (NA) along with pcDNA3.1(+) (Invitrogen), and were cultured in MEM containing 5% NCS

49

and 0.8 mg/ml Geneticin. Surviving cell colonies were picked and were tested for HA and NA expression by means of immunostaining with anti-WSN HA and NA antibodies. Antigen-positive cells were then cloned by using a limited dilution assay. Expression of HA but not NA protein was confirmed in the resulting cell clones. All cells were maintained at 37°C in 5% CO_2. Mouse-adapted CA04 virus (Sakabe et al., 2011) was propagated in MDCK cells as previously described.

Generation of uncleavable HA virus. The uncleavable HA virus was artificially generated by using plasmid-based reverse genetics as described previously (Neumann et al., 1999). This virus was a reassortant between CA04 and A/Puerto Rico/8/34 (PR8) viruses. Briefly, eight PolI plasmids (mutant HA and NA (Sakabe et al., 2011) from CA04 and all others from PR8 (Horimoto et al., 2007) were transfected with five protein-expressing plasmids for the expression of the three polymerases, nucleoprotein (NP) (Horimoto et al., 2007), and wild-type CA04 HA into HEK293T cells. Forty-eight hours after transfection, the supernatants containing the uncleavable HA virus were harvested and propagated once in HA-MDCK (CA04) at a multiplicity of infection (MOI) of 0.001 at 35°C for 48 h in MEM containing L-(tosylamido-2-phenyl) ethyl chloromethyl ketone-treated trypsin (0.8 μg/ml) and 0.3% bovine serum albumin (BSA) (Sigma Aldrich). Cell debris was removed by centrifugation at 3,500 rpm for 20 min at 4°C and the supernatants were stored at -80°C until use.

Preparation of formalin-inactivated virus. For the formalin-inactivated virus, a reassortant virus between CA04 (wild-type HA and NA genes) and PR8 (the rest of the genes) (CA04 2:6 virus) was generated by using plasmid-based reverse genetics as

described above. The virus was propagated in MDCK cells and the culture supernatants containing the virus were treated with 0.1% formalin (final concentration) (Sigma Aldrich) at 4°C for a week to inactivate infectivity. Inactivation of the virus was confirmed by the absence of detectable infectious virus following inoculation of formalin-treated virus into MDCK cells. After confirmation of inactivation of infectivity, formalin-treated virus was purified by sucrose-gradient ultracentrifugation at $100,000 \times g$ for 2 h at 4°C and stored at -80°C until use.

Immunostaining assay. Twenty-four hours after infection with viruses, cells were washed twice with phosphate-buffer saline (PBS) and fixed with 100% methanol for 30 min at room temperature. To detect CA04 HA-expressing cells, these cells were reacted with anti-CA04-HA antibody. To determine the viral titer of the uncleavable HA virus, we conducted the same procedure after performing a plaque assay with HA-MDCK (WSN) cells.

Immunization and protection test. Four-, six-, or eight-week-old female C57BL/6 mice (Japan SLC) were intranasally immunized with 50 µl of 1.7 x 10^5 PFU (equivalent to 16 hemagglutination units (HAU)) of the uncleavable HA virus three times, twice, or once, respectively, at 2-week intervals. As control groups, female C57BL/6 mice (4-week-old) were intranasally immunized with 50 µl of 16 HAU of the formalin-inactivated virus (FI) or with medium three times at 2-week intervals. Three weeks after the final vaccination, six mice per group were euthanized to obtain sera, bronchoalveolar lavage (BAL), and nasal washes. In addition, three mice per group were euthanized to obtain lungs and spleen for detection of viral-specific CD8+ T-lymphocytes. Also three

weeks after the final vaccination, mice were challenged with 10 or 100 times the 50%

mouse lethal dose (MLD_{50}) of mouse-adapted CA04 virus. Eight mice per group were

monitored for survival and body weight changes for 14 days after challenge. Lungs and

nasal turbinates from three mice per each group were collected on days 3 and 6 after

challenge to determine virus titers. Virus titers were determined on MDCK cells.

Detection of virus-specific antibodies. Virus-specific antibodies in nasal wash,

BAL, and serum were detected by using an enzyme-linked immunosorbent assay

(ELISA) (Kida et al., 1982). I used undiluted samples (nasal washes and BAL) and 1:10

diluted samples (serum). In this assay, 96-well ELISA plate wells were coated with

approximately 200 HAU (in 50 μl) of purified CA04 virus treated with disruption buffer

(0.5M Tris-HCl [pH 8.0], 0.6M KCl, and 0.5% Triton X-100). After incubation of the

samples on virus-coated plates, goat anti-mouse IgA or IgG antibody conjugated to

horseradish peroxidase (Kirkegaard & Perry Laboratory Inc) was added to detect bound

antibody.

Detection of virus-specific CD8^{+} T lymphocytes. A tetramer assay was used to

detect virus-specific CD8^{+} T lymphocytes. Single cell suspensions of lung and spleen

were prepared from inoculated mice three weeks after their final vaccination. After being

incubated with anti-CD16/32 (BD Bioscience), the cells were mixed with a Phycoerythrin

(PE)-conjugated H-2D[b] tetramer specific to the NP epitope (amino acid positions 366–

374, ASNENMETM) (MBL) at room temperature for 20 min. Cells were then incubated

with Allophycocyanin-cyanine 7 (cy7)-conjugated anti-CD3ε antibody (BD-Bioscience),

PE-cy7-conjugated anti-CD8α antibody (BD Bioscience), and via-probe (BD Bioscience)

for 30 min at 4°C and then washed with PBS containing 0.5% BSA and 2 mM EDTA (pH 7.2). Cells were analyzed with FACSAria II (Becton, Dickinson and Company) and FlowJo software (Tree Star, Inc.).

Results

Replicative ability and viral protein expression of the uncleavable HA virus in vitro. To generate the uncleavable HA, the arginine at the cleavage site of HA1, which is important for HA cleavage by trypsin-like protease, was changed to threonine. Since the cleavage of HA protein is essential for membrane fusion (Skehel et al., 2000), a virus possessing this uncleavable HA should be unable to complete its replication cycle. To assess this, I examined if the uncleavable HA virus replicated in MDCK and HA-MDCK (CA04) cells: the latter cells constitutively express CA04 virus HA. As expected, CA04 2:6 reassortant virus, serving as a control, replicated to a similar extent in both MDCK and HA-MDCK (CA04) cells (Fig. 1). By contrast, although no infectious particles of the uncleavable HA virus were detected in the supernatant of MDCK cells, the uncleavable HA virus could replicate efficiently in HA-MDCK (CA04) cells, to a level comparable to that of CA04 2:6 reassortant virus (Fig. 1). I also tested whether the virus could revert to the wild-type by passaging it in MDCK cells. After three passages, I did not observe any cytopathic effect (data not shown), suggesting that the mutation was stable.

To further ensure that the uncleavable HA virus replicated in HA-MDCK cells, but not in MDCK cells, I visualized the infected cells by immunostaining (Fig. 2). Whereas CA04 2:6 virus efficiently spread in both cell types (Fig. 2, left panels), the uncleavable HA virus only infected and expressed viral protein (HA in this case) in individual MDCK cells (Fig. 2, upper middle panel) although it efficiently spread in HA-MDCK (WSN) cells (Fig. 2, lower middle panel). These results indicate that the uncleavable HA virus is replication-incompetent, capable of only a single cycle of

54
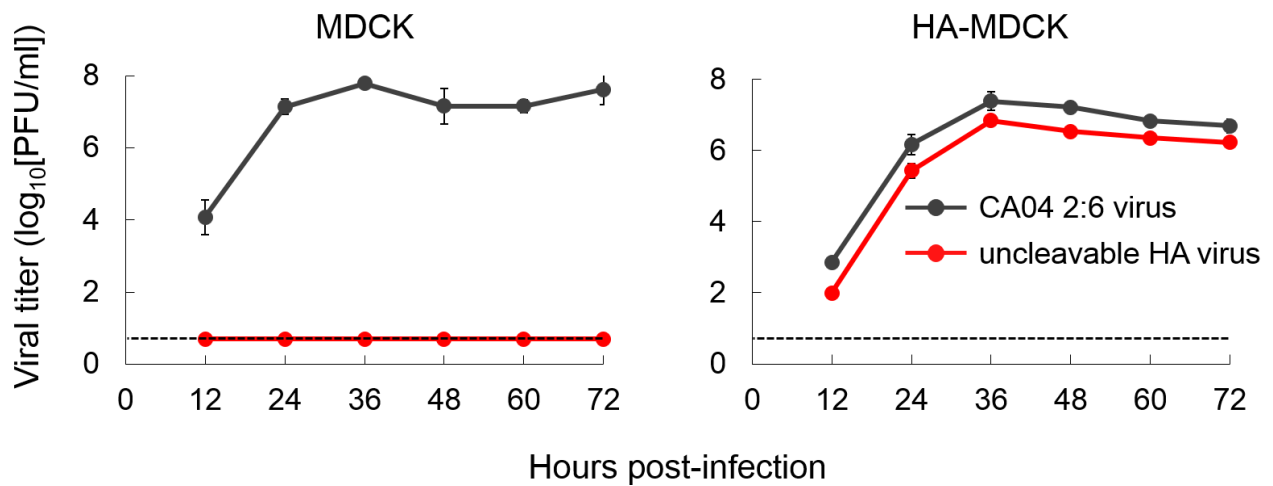
Fig. 1. Growth kinetics of CA04 2:6 and uncleavable HA viruses in MDCK and HA-MDCK cells.

  Both cell types were infected with viruses at an MOI of 0.001. Supernatant was collected every 12 h, and viral titers in the supernatants of both cell types were determined by means of the conventional plaque assay or a plaque assay with immunostaining with an anti-HA antibody using HA-MDCK cells. The broken line indicates the detection limit for virus titers (5 PFU/ml).
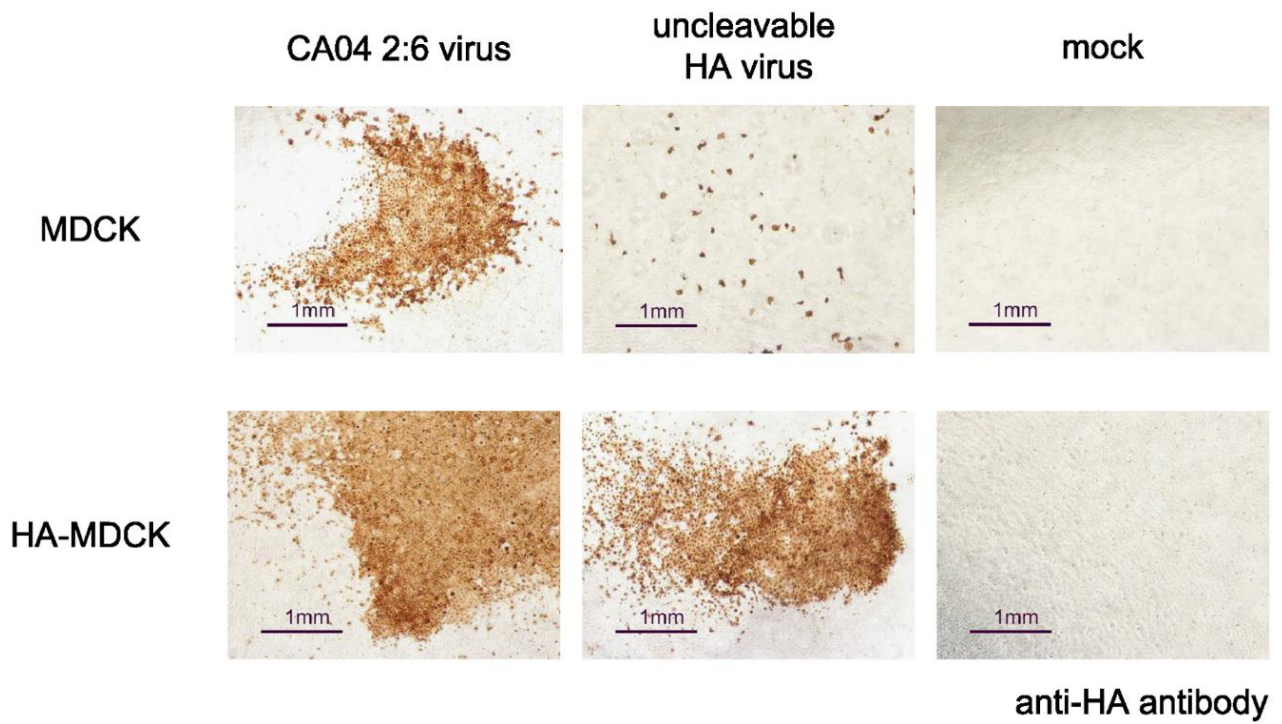
Fig. 2. HA protein expression in virus-infected cells.

MDCK and HA-MDCK (WSN) cells were infected with CA04 2:6 and uncleavable HA

viruses; 24 h after infection, the cells were fixed and stained by using an anti-CA04 HA

antibody. Cells colored brown are CA04 HA-expressing cells.

infection and unable to produce infectious progeny in normal MDCK cells.

Induction of virus-specific immunity by the uncleavable HA virus in mice. To assess the ability of the uncleavable HA virus to induce virus-specific immunity against influenza virus, I immunized mice with the uncleavable HA virus or FI. To examine virus-specific antibody production, IgG and IgA against CA04 in the nasal wash, BAL, and serum of immunized mice were measured by using an ELISA (Fig. 3). Although only low levels of antibodies were detected in mice immunized three times with FI or inoculated with medium, antibody levels increased as the number of vaccinations increased in mice immunized with the uncleavable HA virus. Notably, both the virus-specific IgG and IgA titers in BAL, and the IgG in serum from mice immunized only once with the uncleavable HA virus were higher than the respective titers from mice immunized with FI three times.

I also examined the virus-specific (NP in this case) CD8$^+$ T cell response by using a tetramer assay. NP-specific CD8$^+$ T cells were identified in the lungs and spleens only of mice immunized with the uncleavable HA virus (Fig 4). Of note, NP-specific CD8$^+$ T cells predominantly accumulated in the lungs rather than the spleens of the immunized mice (Fig. 4), and the number of NP-specific CD8$^+$ T cells increased as the number of vaccinations increased (Fig. 4B).

These results demonstrate that the uncleavable HA virus could elicit both humoral and cellular immunity more efficiently than FI against influenza virus at the local sites where influenza virus replicates.
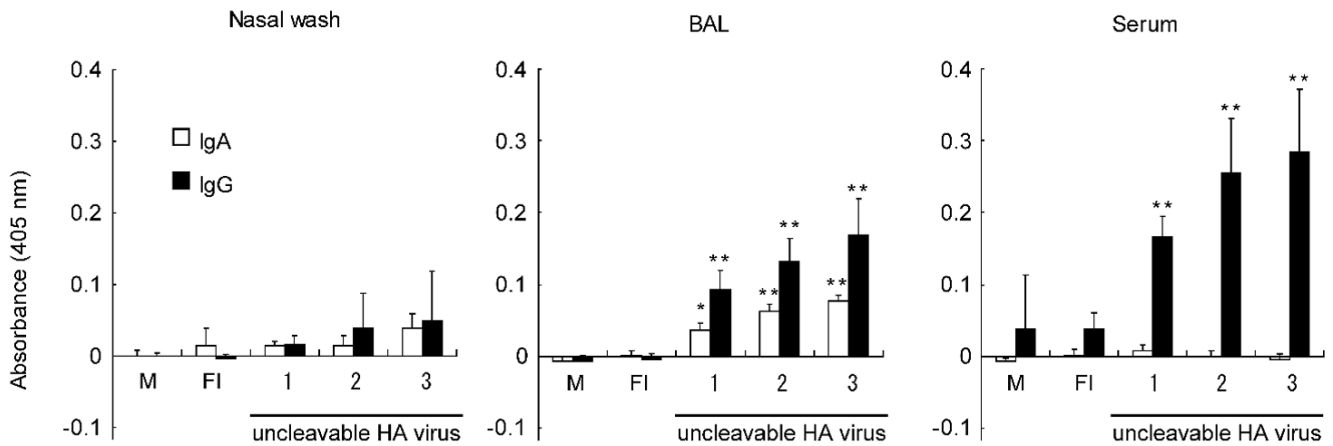
Fig. 3. Induction of virus-specific IgG and IgA in nasal wash, BAL, and serum of mice immunized with the uncleavable HA virus.

Virus-specific antibodies were detected by means of an ELISA. Samples from six mice from each group were obtained 3 weeks after the final vaccination. Results are expressed as the mean absorbance ($\pm$ standard deviations) of undiluted samples (nasal wash and BAL) or of 1:10 diluted samples (serum). Statistically significant differences among the groups were assessed by using the Tukey-Kramer method. Asterisks (* or **) indicate a significant difference from samples from mice inoculated with FI (*, $P<0.05$; **, $P<0.01$). The numbers on the x-axis indicate the times of vaccination of uncleavable HA virus. M: medium. FI: Mice were immunized with formalin-inactivated vaccine three times with 2 week intervals.
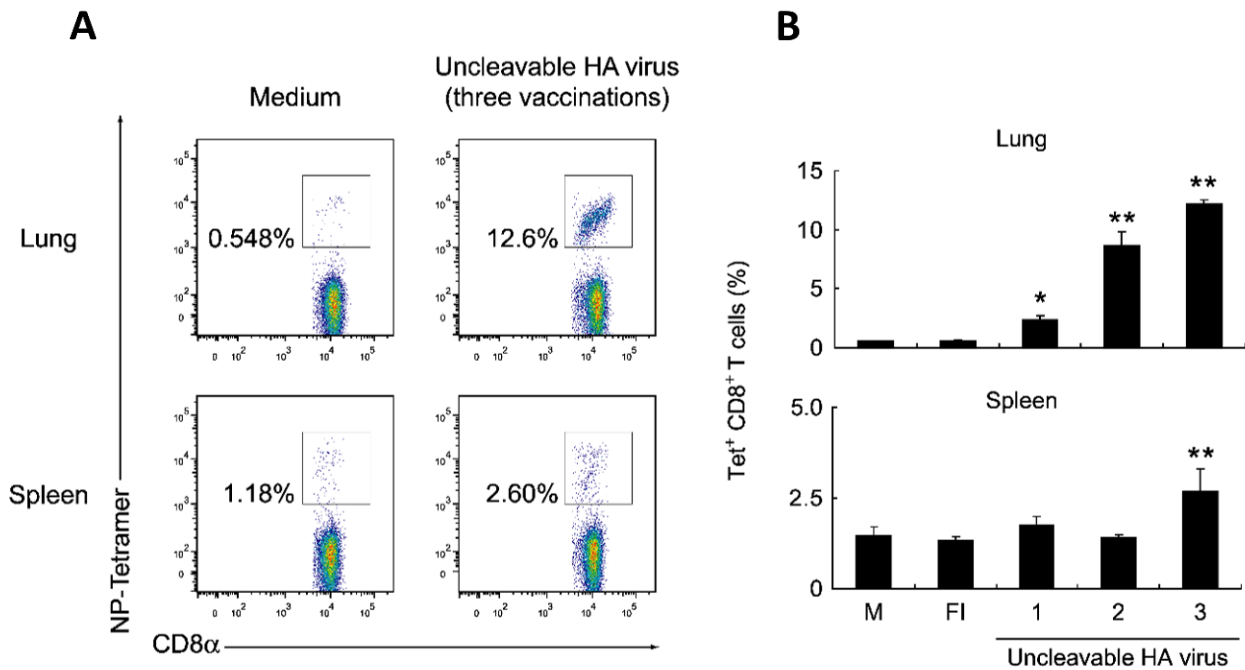
Fig. 4. Induction of virus-specific CD8$^+$ T cells in mice immunized with the uncleavable HA virus.

Virus-specific CD8$^+$ T cells were detected in the lungs and spleen of inoculated mice by using a tetramer assay. (A) Representative dot plot for CD3ε$^+$ CD8α$^+$ cells from the spleen or lungs of a mouse inoculated with medium or with the uncleavable HA virus. (B) The percentage of virus-specific CD8$^+$ T cells (NP-tetramer$^+$ CD8α$^+$ population) in the CD3ε$^+$ CD8α$^+$ cell populations in the lungs and spleen of inoculated mice. Results are expressed as the mean values (± standard deviations). Statistically significant differences among the groups were assessed by using the Tukey-Kramer method. Asterisks (* or **) indicate significant differences from samples from mice inoculated with FI (*, $P<0.05$; **, $P<0.01$).

Protection against influenza virus in mice immunized with the uncleavable HA virus. Finally, I evaluated the protective ability of the uncleavable HA virus. To this end, I monitored body weight changes and survival of mice immunized with the uncleavable HA virus after challenge. The body weights of mice inoculated with medium decreased rapidly to approximately 70%−80% (Fig. 5A) and most mice (7 out of 8) succumbed to their infection (Fig. 5B). The body weights of mice immunized with FI also clearly decreased to 80% (Fig. 5A) and several mice (3 and 5 out of 8 with 10 and 100 MLD_{50}, respectively) died (Fig 5B). By contrast, with 10 MLD_{50}, mice immunized once with the uncleavable HA virus showed slightly reduced body weights, and mice immunized twice and three times with this virus showed no body weight changes (Fig. 5A left panel). Moreover, all mice immunized with this virus survived (Fig. 5B left panel). With 100 MLD_{50}, although mice immunized once with this virus showed similar body weight reductions as mice immunized with medium and FI, the mice immunized twice and three times with the uncleavable HA virus showed only slight or no body weight loss, respectively (Fig. 5A, right panel). All mice immunized with the uncleavable HA virus survived, except for 3 out of 8 mice immunized only once with the uncleavable HA virus (Fig. 5B, right panel).

I also determined virus titers in the lungs and nasal turbinates of mice immunized with the uncleavable HA virus after challenge (Table 1). Virus titers in both organs of mice immunized with the uncleavable HA virus were appreciably lower as the number of vaccinations increased, especially on day 6 post-infection, than those in organs of mice immunized with medium or with FI. Taken together, these results indicate that the uncleavable HA virus has potency as an influenza vaccine.
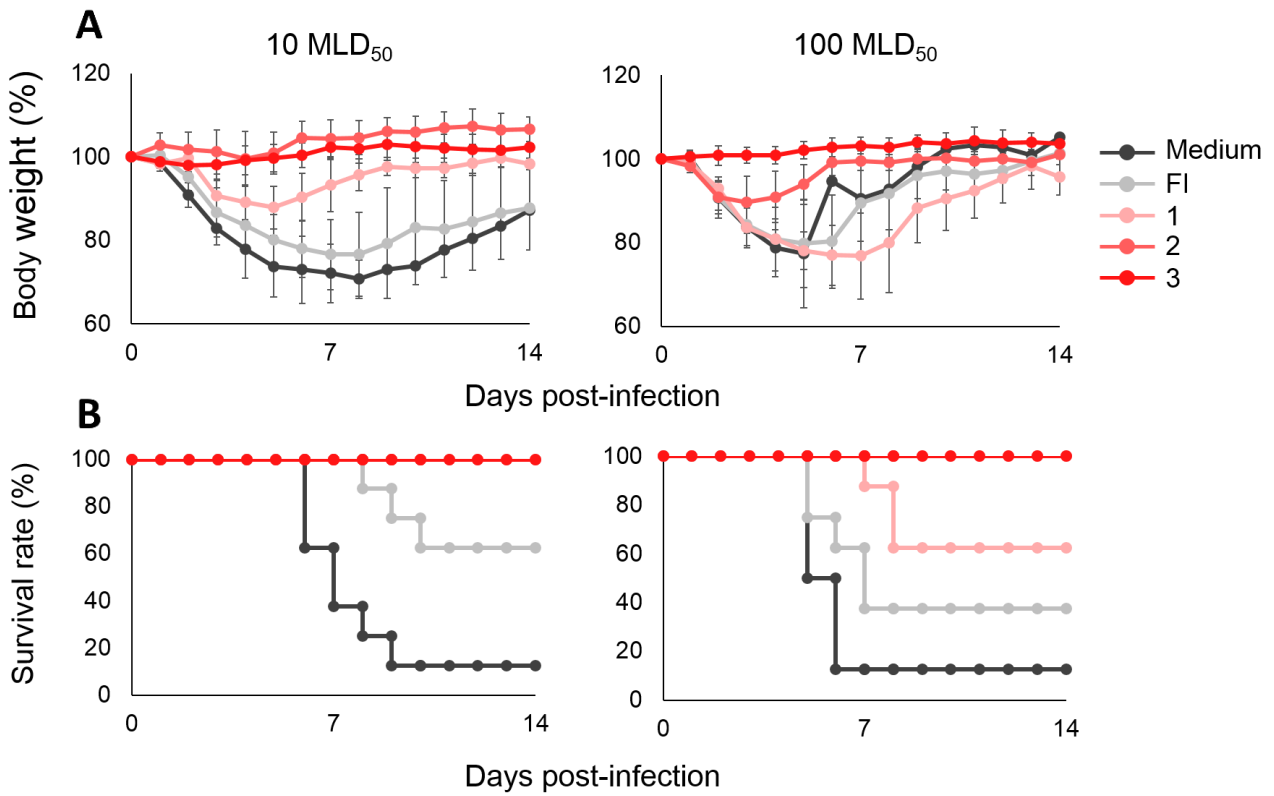
Fig. 5. Body weight changes and survival curves for mice challenged with wild-type virus.

Eight mice per group were intranasally challenged with 10 or 100 MLD_{50} of mouse-adapted CA04 3 weeks after the final vaccination. Body weights were measured (A) and survival rate was monitored (B) for 14 days after challenge.

Table. 1. Protection against challenge with lethal doses of influenza virus in mice immunized with an uncleavable HA virus[a]

challenge dose	inoculum	days post-infection	organ	Virus titer (mean ±SD log$_{10}$[PFU/g])	challenge dose	inoculum	days post-infection	organ	Virus titer (mean ±SD log$_{10}$[PFU/g])
10MLD$_{50}$	Medium	3 dpi	NT[b]	5.1 ± 0.6	100MLD$_{50}$	Medium	3 dpi	NT	5.7 ± 0.4
			Lung	7.0 ± 0.4				Lung	7.5 ± 0.2
		6 dpi	NT	4.2 ± 0.3			6 dpi	NT	NA[c]
			Lung	6.4 ±0.4				Lung	NA
	FI[d]	3 dpi	NT	4.6 ± 0.5		FI	3 dpi	NT	5.7 ± 0.7
			Lung	7.3 ± 0.0				Lung	7.1 ± 0.7
		6 dpi	NT	4.0 ± 0.2			6 dpi	NT	3.9 ± 0.5
			Lung	6.0 ± 0.3				Lung	5.3 ± 0.4
	Once	3 dpi	NT	5.2, 5.8		Once	3 dpi	NT	4.9 ± 0.4
			Lung	7.8 ± 0.2				Lung	7.5 ± 0.5
		6 dpi	NT	ND[e]			6 dpi	NT	3.3, 3.5
			Lung	3.4, 3.2				Lung	3.7 ± 2.3
	Twice	3 dpi	NT	4.3, 3.9		Twice	3 dpi	NT	6.0
			Lung	6.1 ± 0.8				Lung	1.6, 6.5
		6 dpi	NT	ND			6 dpi	NT	1.6
			Lung	2.5, 2.5				Lung	ND
	Three times	3 dpi	NT	ND		Three times	3 dpi	NT	ND
			Lung	2.2				Lung	5.8, 2.4
		6 dpi	NT	ND			6 dpi	NT	ND
			Lung	2.0				Lung	ND

[a] Twelve mice from each group were intranasally inoculated with 10 or 100 MLD$_{50}$ of mouse-adapted CA04 (50 μl per mouse) 3 weeks after the final vaccination. Three mice per group were sacrificed on days 3 and 6 post-infection, and lungs and nasal turbinate were collected to determine virus titers. Results are expressed as the mean titer (log$_{10}$ PFU/g) ± standard deviations. When virus was not recovered from all three mice,

individual titers are given.

[b] NT: Nasal turbinate

[c] NA: Not applicable because the mice died

[d] FI: formalin-inactivated virus. Mice were immunized three times with two week intervals.

[e] ND: Not detected (detection limit, 10 PFU/lung or 5 PFU/NT)

Discussion

Currently, embryonated hen's eggs are typically used to produce both inactivated and live-attenuated vaccines, although cell-based vaccines are approved in Europe. However, vaccine production in eggs has several issues. One problem is the alteration of antigenicity from that of the circulating virus during cultivation of the vaccine strain in embryonated hen's eggs (Katz et al., 1987; Newman et al., 1993; Williams et al., 1993). Another is allergic reactions to components derived from eggs present in vaccines grown in eggs (Gruenberg et al., 2011). In contrast, the antigenicity of viruses grown in cells closely matches that of viruses isolated from influenza patients (Williams et al., 1993; Katz et al., 1989). Since the uncleavable HA virus in this study only grew in HA-expressing cells and to a level comparable to a virus possessing wild-type HA (Fig. 1), production of this vaccine should not only be feasible, but this type of vaccine should maintain its antigenicity; however, the cell line needs to be validated to ensure that it is free of anything harmful, such as tumorigenicity.

I demonstrated that antibody responses (IgA and IgG) were efficiently induced by the uncleavable HA virus (Fig. 3), like NS2-knockout VLPs (Watanabe et al., 2002). In addition to antibody responses, I tested the virus-specific CTL response, which we did not examined with our NS2-knockout VLPs, and found that a CTL response to an internal viral protein (i.e., NP) was also induced by this virus (Fig. 4). The reason for this induction is that viral proteins (NP in this case) are expressed in cells infected with this replication-incompetent virus, suggesting that this virus could act similarly to a live-attenuated virus in terms of induction of immunity despite not generating infectious progeny.

My findings suggest that a combination of this type of virus and cells expressing

a seasonal virus HA can serve as a platform for a bivalent vaccine as follows: If an uncleavable H5 HA gene is partnered with the rest of the genes from a seasonal influenza virus, the resulting virus can serve as a vaccine against H5 and seasonal influenza viruses. That is, antibody responses against H5 HA (expressed from the viral HA gene) and HA (derived from the cell line) would likely be induced as would CTL responses against H5 HA and the internal viral proteins (expressed from the genes of the seasonal virus). Likewise, if a gene, encoding a protein responsible for inducing immunity, from another respiratory pathogens, such as *Streptococcus pneumoniae*, which causes secondary bacterial infections following influenza virus infection, or respiratory syncytial virus, which causes severe manifestations in infants, is inserted into the HA gene, the resultant virus may be used as a vaccine against both influenza virus and the other respiratory pathogen.

In conclusion, a replication-incompetent virus that possesses a modified HA gene, when partnered with an HA-expressing cell line, has potential as a novel vaccine candidate.

CHAPTER III

A bivalent vaccine based on a replication-incompetent influenza virus protects against *Streptococcus pneumoniae* and influenza virus infection.

Abstract

Streptococcus pneumoniae (*S. pneumoniae*) is a major causative pathogen in community-acquired pneumonia; together with influenza virus, it represents an important public health burden. Although vaccination is the most effective prophylaxis against these infectious agents, no single vaccine simultaneously provides protective immunity against both *S. pneumoniae* and influenza virus. Previously, we demonstrated that several replication-incompetent influenza viruses efficiently elicit IgG in serum and IgA in the upper and lower respiratory tracts. Here, I generated a replication-incompetent hemagglutinin-knockout (HA-KO) influenza virus possessing the sequence for the antigenic region of pneumococcal surface protein A (PspA). Although this virus (HA-KO/PspA virus) could replicate only in an HA-expressing cell line, it infected wild-type cells and expressed both viral proteins and PspA. PspA- and influenza virus-specific antibodies were detected in nasal wash, bronchoalveolar lavage fluid, and serum from mice intranasally inoculated with HA-KO/PspA virus, and mice inoculated with HA-KO/PspA virus were completely protected from lethal challenge with either *S. pneumoniae* or influenza virus. Further, bacterial colonization of the nasopharynx was prevented in mice immunized with HA-KO/PspA virus. These results indicate that HA-KO/PspA virus is a promising bivalent vaccine candidate that simultaneously confers protective immunity against both *S. pneumoniae* and influenza virus. I believe that this strategy offers a platform for the development of bivalent vaccines, based on replication-incompetent influenza virus, against pathogens that cause respiratory infectious diseases.

Introduction

Streptococcus pneumoniae (*S. pneumoniae*) is a Gram-positive aerobic bacterial species for which there are more than 90 serotypes based on the chemical and serological features of its capsular polysaccharides. *S. pneumoniae* is a common cause of community-acquired pneumonia, and its colonization of the nasopharynx always precedes infections such as otitis media, sinusitis, pneumonia, and meningitis (Bogaert et al., 2004; Jambo et al., 2010; Kadioglu et al., 2008; McCullers et al., 2006).

Two main types of vaccine against *S. pneumoniae* are available: a twenty three-valent pneumococcal polysaccharide vaccine (PPV23), and a heptavalent pneumococcal conjugated vaccine (PCV7). These vaccines contain *S. pneumoniae* polysaccharides that are selected on the basis of the epidemic situation. Although several studies have demonstrated the protective efficacy of these vaccines, they are ineffective against serotypes that were not included in the vaccines. Therefore efforts are ongoing to develop a vaccine that is effective regardless of serotype. Several proteins that are expressed on the surface of the bacteria, such as choline-binding protein A and pneumococcal surface adhesin A are considered attractive antigens for a new vaccine (Bogaert et al., 2004; Jambo et al., 2010; Moffitt et al., 2011; Rodgers et al., 2011). Among them, PspA is thought to be particularly promising. PspA is found in all clinical *S. pneumoniae* isolates (Jedrzejas et al., 2007). Some studies have demonstrated that antibodies against PspA neutralize the anticomplement effect of PspA, which results in clearance of bacteria by depositing complement C3 on the bacterial surface (Ochs et al., 2008; Ren et al., 2004). Moreover, anti-PspA antibodies have also been shown to prevent infection from strains with different serotypes (Nabors et al., 2000). It has been reported that mice immunized

68

with recombinant PspA protein in combination with polyinosinic-polycytidylic acid (poly(I:C)), Toll-like receptor (TLR) agonist, as an adjuvant, were completely protected against secondary pneumococcal pneumonia after influenza virus infection (Ezoe et al., 2011), and in human trials, intramuscular immunization with the recombinant PspA protein induced cross-reactive antibodies to heterologous PspA (Nabors et al., 2000).

Influenza virus also causes serious respiratory infections, and inactivated and live-attenuated influenza vaccines are approved for prophylaxis against influenza. Although inactivated vaccines are highly safe and induce IgG in sera, they cannot elicit secretory IgA at the mucosal surface of the respiratory tract where influenza virus replicates. Intranasal administration of live-attenuated vaccines, which carry mutations that lead to temperature sensitivity and viral attenuation, induces not only IgG in sera, but also IgA at the mucosal surface. However, live-attenuated vaccines are not recommended for children under the age of 2, adults aged 50 or over, immunocompromised patients, or pregnant women, because of safety concerns of the replication of the vaccine virus (Ambrose et al., 2008; Cox et al., 2004; Fiore e al., 2010). To overcome these limitations, efforts are ongoing to develop an ideal influenza vaccine that is highly safe and induces secretory IgA at the mucosal surface of the respiratory tract.

As described in CHAPTER III, I established a replication-incompetent influenza virus that possesses a hemagglutinin (HA) that is not cleaved into HA 1 and HA 2 by proteases (uncleavable HA virus) (Katsura et al., 2012). I demonstrated that this uncleavable HA virus could infect and express viral protein in wild-type cells, but does not produce infectious progeny viruses in these cells; however, it could induce virus-specific humoral and cellular immunity in the respiratory tracts of immunized mice. Given that this replication-incompetent virus can be propagated in an HA-expressing cell

69

line, this system could be used to generate bivalent vaccines in which the antigen gene of another respiratory pathogen is introduced into the HA gene. To assess this possibility, here I generated HA-knock out (KO) PspA virus as a bivalent vaccine candidate, possessing the PspA antigen gene instead of the HA gene, and examined its immunogenicity and vaccine efficacy against both influenza virus and *S. pneumoniae* in mice.

Material and Methods

Cells. Madin-Darby canine kidney (MDCK) cells were maintained in minimum essential medium (MEM) containing 5% of newborn calf serum (NCS). Human embryonic kidney 293T (HEK293T) cells were maintained in Dulbecco's modified Eagle medium supplemented with 10% fetal calf serum. MDCK cells expressing HA (HA-MDCK) were established by co-transfection with plasmids for the expression of HA derived from A/Puerto Rico/8/34 (PR8) and puromycin *N*-acetyltransferase as previously described (Katsura et al., 2012). HA-MDCK cells were cultured in MEM containing 5% NCS and 5 µg/ml puromycin dihydrochloride (Nacalai Tesque).

Preparation of virus and bacteria. PR8 was generated by using reverse genetics (Neumann et al., 1999) and propagated in MDCK cells at 37°C. Forty-eight hours after infection, the supernatants were harvested and stored at -80°C until use. *S. pneumoniae* WU2 strain with serotype 3 and EF3030 strain with serotype 19F, which is virulent and relatively avirulent in mice, respectively (Briles et al., 2003; Briles et al., 2005) were grown in Todd-Hewitt Broth (Becton Dickinson) supplemented with 0.5% yeast extract (THY) to mid-log phase and washed twice with Dulbecco's phosphate-buffered saline (PBS) without $CaCl_2$ and $MgCl_2$ (Sigma-Aldrich). Bacteria were then suspended in THY containing 10% glycerol, and the aliquots of bacteria were stored at -80˚C until use.

Plasmid construction. For viral RNA (vRNA) expression, plasmids containing the cDNAs of PR8 genes between the human RNA polymerase I promoter and the mouse

71

RNA polymerase I terminator (referred to as PolI plasmid) were generated. To generate plasmids that express the PspA antigenic region or green fluorescent protein (GFP) from the HA segment, I utilized the packaging signal of the HA segment of influenza virus (Watanabe et al., 2003). Plasmids (pPolI-HA(9)PspA(80) and pPolI-HA(9)GFP(80)) were constructed to replace the PolI plasmid that encoded the HA segment of PR8. These plasmids contained the 3' HA non-coding region, 9 nucleotides that correspond to the HA-coding sequence at the 3' end of the vRNA followed by the PspA antigenic region of the Rx1 strain (serotype 2) (amino acid positions 32–333) or the GFP-coding sequence, 80 nucleotides that correspond to the HA-coding sequence at the 5' end of the vRNA, and lastly the 5' HA non-coding region. The sequences were determined to ensure that no unwanted mutations were introduced.

Plasmid-driven reverse genetics. To generate the viruses that possess the HA segment encoding the PspA antigenic region (HA-KO/PspA virus) or GFP (HA-KO/GFP virus), I used plasmid-driven reverse genetics as described previously (Neumann et al., 1999). Briefly, pPolI-HA(9)PspA(80) or pPolI-HA(9)GFP(80) and the remaining 7 PolI plasmids were cotransfected into HEK293T cells together with eukaryotic protein expressing plasmids for PB2, PB1, PA, NP, and wild-type HA derived from PR8 by using the TransIT-293 transfection reagent (Mirus). Forty-eight hours after transfection, the supernatants containing the HA-KO/PspA virus or the HA-KO/GFP virus were harvested and propagated once in HA-MDCK cells at 37°C for 48 h in MEM containing L-(tosylamido-2-phenyl) ethyl chloromethyl ketone-treated trypsin (0.8μg/ml) and 0.3% bovine serum albumin (BSA) (Sigma Aldrich). Cell debris was removed by centrifugation at 2,100 x *g* for 20 min at 4°C, and the supernatants were stored at -80°C until use. The

virus titers were determined by counting cells expressing PspA or GFP by immunostaining or fluorescence observation, respectively, after a plaque assay using HA-MDCK cells.

Western blot analysis. Western blotting was performed as described previously (Gorai et al., 2012) with modifications. A549 cells were infected with HA-KO PspA virus or HA-KO GFP virus at a multiplicity of infection (MOI) of 10 without trypsin. Twenty-four hours after infection, the cells were lysed with Novex® Tris-Glycine SDS sample buffer (Invitrogen) and subjected to SDS-polyacrylamide gel electrophoresis in Novex® Tris-Glycine SDS running buffer (Invitrogen). After electrophoresis, the proteins were transferred to a PVDF membrane in transfer buffer (100mM Tris, 190 mM glycine). The membrane was steeped in Blocking One (Nacalai Tesque) for 1 h. Then, the membrane was incubated with a mouse anti-PspA antibody, rabbit antiserum that reacts with influenza viral proteins, or a mouse anti-β-actin antibody. After incubation with the primary antibodies followed by washing with PBS containing 0.05% Tween-20 (PBS-T), the membrane was incubated with horseradish peroxidase conjugated species-specific secondary antibodies (GE Healthcare). Finally, specific proteins were detected using the ECL Plus Western Blotting Detection System (GE Healthcare). The VersaDoc Imaging System (Bio-Rad) was used to obtain photographic images.

Immunofluorescence assay. MDCK and HA-MDCK cells were infected with PR8 or HA-KO/PspA virus at an MOI of 0.0001. Twelve hours after infection, the cells were washed twice with PBS and fixed with 4% paraformaldehyde for 10 minutes. After permeabilization with PBS containing 0.2% Triton X-100, the cells were incubated with

a mouse anti-PspA antibody or with rabbit antiserum against influenza viral proteins. Goat anti-mouse IgG Alexa 488 and anti-rabbit IgG Alexa 594 (molecular probes) served as secondary antibodies. Cells were observed by fluorescence microscopy.

Immunization and protection test. Seven-week-old female C57BL/6 mice (Japan SLC) were intranasally inoculated with 50 μl of 10^5 plaque-forming units (PFU) of HA-KO/PspA virus twice, with a 2-week interval between the inoculations. As control groups, age-matched female C57BL/6 mice were intranasally inoculated with 50 μl of 10^5 PFU of HA-KO/GFP virus or medium on the same schedule. Two weeks after the final vaccination, six mice per group were euthanized to obtain sera, bronchoalveolar lavage fluid (BALF), and nasal washes. Also two weeks after the final vaccination, mice were challenged with 100 times the 50% mouse lethal dose (MLD_{50}) of PR8 virus. Eight mice per group were monitored for survival and body weight changes for 14 days after PR8 challenge. Lungs and nasal turbinates from three mice per group were collected on days 3 and 6 after challenge to determine virus titers. Virus titers were determined on MDCK cells. In addition, two weeks after the final vaccination, mice were intranasally challenged with 3 MLD_{50} of *S. pneumoniae* WU2 strain. Ten mice per group were monitored for survival for 14 days after challenge. Similarly, two weeks after the final vaccination, mice were intranasally challenged with 1.0 x 10^2 colony-forming units (cfu) of *S. pneumoniae* EF3030 strain. Nasal washes from ten mice per group were collected on day 5 after challenge to determine the bacterial clearance from the nasopharynx. The quantitative bacterial culture of the nasal washes was performed.

Detection of pathogen-specific antibodies. Pathogens-specific antibodies in nasal washes, BALF, and serum were detected by means of an enzyme-linked immunosorbent assay (ELISA) (Kida et al., 1982). To detect virus-specific antibodies, I used 2-fold serially diluted serum, BALF, and nasal washes. In this assay, 96-well ELISA plate wells were coated with approximately 200 hemagglutination unit (in 50 μl) of purified PR8 virus treated with disruption buffer (0.5M Tris-HCl [pH 8.0], 0.6M KCl, and 0.5% Triton X-100). After the diluted samples were incubated on the virus-coated plates for 1 h at room temperature, goat anti-mouse IgA or IgG antibody conjugated to horseradish peroxidase (Kirkegaard & Perry Laboratory Inc.) was added to detect bound antibody. The optical density (OD) was measured at 405 nm with a microplate reader. End-point titers are expressed as the reciprocal $\log_2$ of the last dilution whose OD value was more than the cut-off value. The cut-off value was determined by adding threefold standard deviations (SD) to the mean (i.e., mean + 3 SD) of the OD values of samples from naïve mice.   PspA-specific antibody titers in nasal washes, BALF, and serum were determined by use of an ELISA as previously described (Ezoe et al., 2011). Microtiter plates were coated overnight at 4 °C with 100 μl of 1 μg/ml of PspA. The plates were then washed with PBS-T. Serially diluted nasal washes, BALF, and serum (50 μl) was added to the plates, and the plates were then incubated for 30 min at 37 °C. The plates were washed three times with PBS-T and incubated with alkaline phosphatase-conjugated goat anti-mouse IgG, IgG1, IgG2a or IgA (Zymed) for 30 min at 37 °C. After this incubation, the plates were washed three times with PBS-T, 4-nitrophenyl phosphate disodium salt hexahydrate (Sigma–Aldrich) diluted with substrate buffer (1M diethanolamine, 0.5 mM $MgCl_2$) was added, and the plates were incubated for 30 min at room temperature in the dark. The OD at 405 nm was then measured with a microplate

reader (Bio-Rad Laboratories). The end-point titers were expressed as the reciprocal $\log_2$ of the last dilution giving 0.1 OD unit of OD_{405} above the OD_{405} of negative control samples obtained from non-immunized mice.

Results

        PspA and GFP expression in infected cells. To examine whether PspA was expressed in HA-KO/PspA virus-infected cells, I infected MDCK and HA-MDCK cells with HA-KO/PspA virus and attempted to detect PspA in virus-infected cells by use of an immunofluorescence assay. PR8 served as a control. PspA expression was detected in both cell types infected with HA-KO/PspA virus, but not in cells infected with PR8 (Fig. 1A). Although HA-KO/PspA virus could efficiently spread and express its viral proteins and PspA in HA-MDCK cells, the infection of HA-KO/PspA virus did not spread in MDCK cells (Fig. 1A). In both cell types infected with HA-KO/PspA virus, I found some cells that expressed the viral proteins, but not PspA (Fig. 1A, white arrows). This may be because the HA segment encoding the PspA antigenic region was not incorporated into the virus particles that infected those cells. This is not surprising since even not all virions contain authentic viral RNA segments (Martin et al., 1991). I also tested whether PspA was expressed in A549 cells infected with HA-KO PspA virus by use of western blotting. PspA was detected in cells infected with HA-KO PspA virus, but not in cells infected with PR8 (Fig. 1B). The M1 protein of influenza virus and β-actin were detected as controls of viral and cellular proteins, respectively. Taken together, these results indicate that HA-KO/PspA virus is replication-incompetent, but can express not only viral proteins but also PspA in virus-infected cells. We obtained similar results with HA-KO/GFP virus (data not shown).
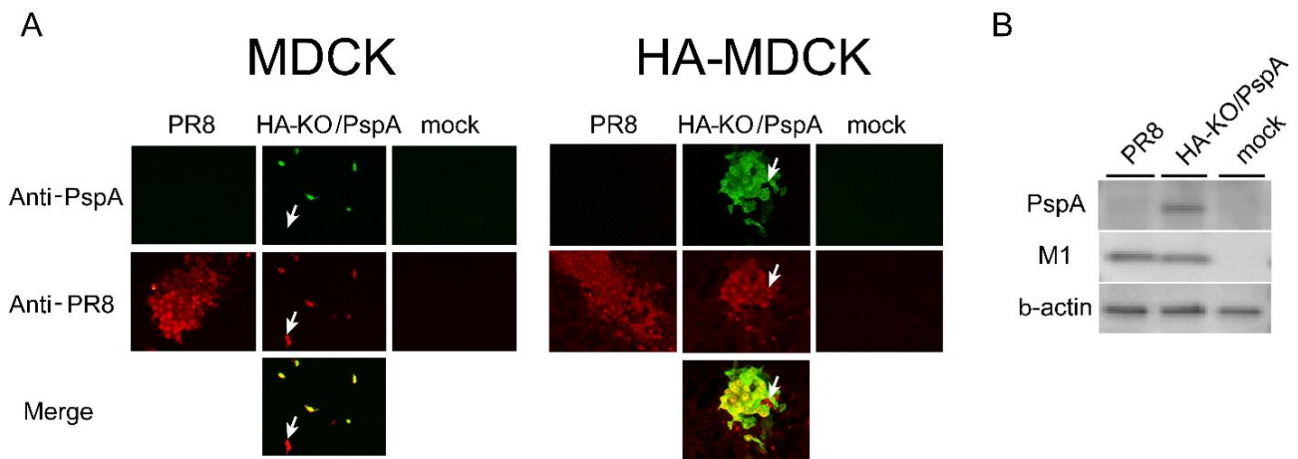
Fig. 1. Expression of the PspA antigenic region and viral proteins in cells infected with PR8 or HA-KO PspA virus.

(A) MDCK and HA-MDCK cells were infected with the respective virus at an MOI of 0.0001, and an immunofluorescence assay was performed 12 h post-infection. PspA (green) and viral proteins (red) were detected by anti-PspA and anti-PR8 antibodies, respectively. White arrows indicate cells that express the viral proteins but not the PspA protein. (B) A549 cells were infected with the respective virus at an MOI of 10, and western blotting was performed 24 h post-infection.

Induction of antibodies against PspA and influenza virus by HA-KO/PspA virus. To assess the ability of HA-KO/PspA virus to induce antibodies against both PspA and PR8, mice were intranasally inoculated twice with 10^5 PFU of HA-KO/PspA virus. Mice inoculated with HA-KO/GFP virus or medium served as controls. Two weeks after the final vaccination, nasal washes, BALF, and serum were collected and subjected to ELISA to measure antigen-specific IgG and IgA in these samples. The induction of IgG against PR8 was detected in serum samples from mice inoculated with HA-KO/PspA or HA-KO/GFP virus (Fig. 2A). Moreover, both IgG and IgA against PR8 were detected in nasal washes and BALF from these mice, although IgA in the nasal washes of mice inoculated with HA-KO/PspA virus was not significantly induced compared with one in the nasal washes of mice inoculated with medium (Figs. 2B and C). These results indicate that the HA-KO/PspA and HA-KO/GFP viruses elicited both virus-specific mucosal and systemic immunity. On the other hand, for the antibody response to PspA, both IgG and IgA titers in the BALF and IgG titers in the serum and nasal washes significantly increased only in mice inoculated with HA-KO/PspA virus (Figs. 3A, B, and C). Likewise, PspA-specific IgG1 and IgG2a titers were also elevated in the serum of these mice (Figs. 3D). While both isotypes inhibit the anticomplement effect of PspA, the complement-fixing ability of IgG2a is superior to that of other isotypes (Ferreira et al., 2008). Therefore, the increase in IgG2a titer in mice inoculated with HA-KO/PspA represents a significant response in terms of the efficient clearance of *S. pneumoniae* via opsophagocytic killing. A PspA-specific antibody response was not observed in samples from mice inoculated with HA-KO/GFP virus or medium. These results indicate that HA-KO/PspA virus can induce a significant antibody response against both influenza virus and PspA at the mucosal surface of the respiratory tract and in blood.

79
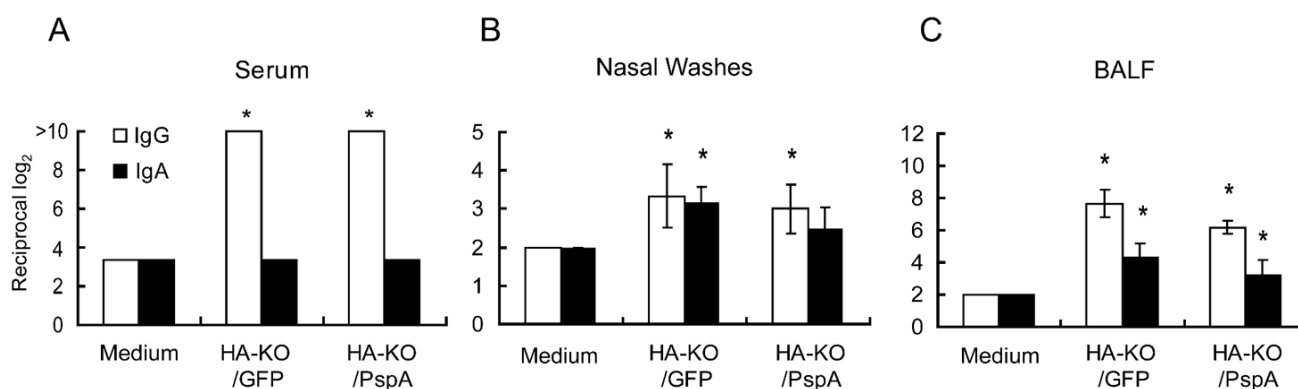
Fig. 2. Induction of influenza virus-specific IgG and IgA in serum (A), nasal washes (B), and BALF (C).

Mice were intranasally inoculated with medium, HA-KO GFP virus, or HA-KO PspA virus with a two-weeks interval between the inoculations. Samples from six mice from each group were collected two weeks after the final vaccination. Virus-specific antibodies were detected by using an ELISA. Results are expressed as the means of the reciprocal titer $\log_2$ ($\pm$ standard deviations (SD)). Statistically significant differences between groups were determined by using the Dunnet method. The asterisk indicates a significant difference from samples taken from mice inoculated with medium (*, $P<0.05$).
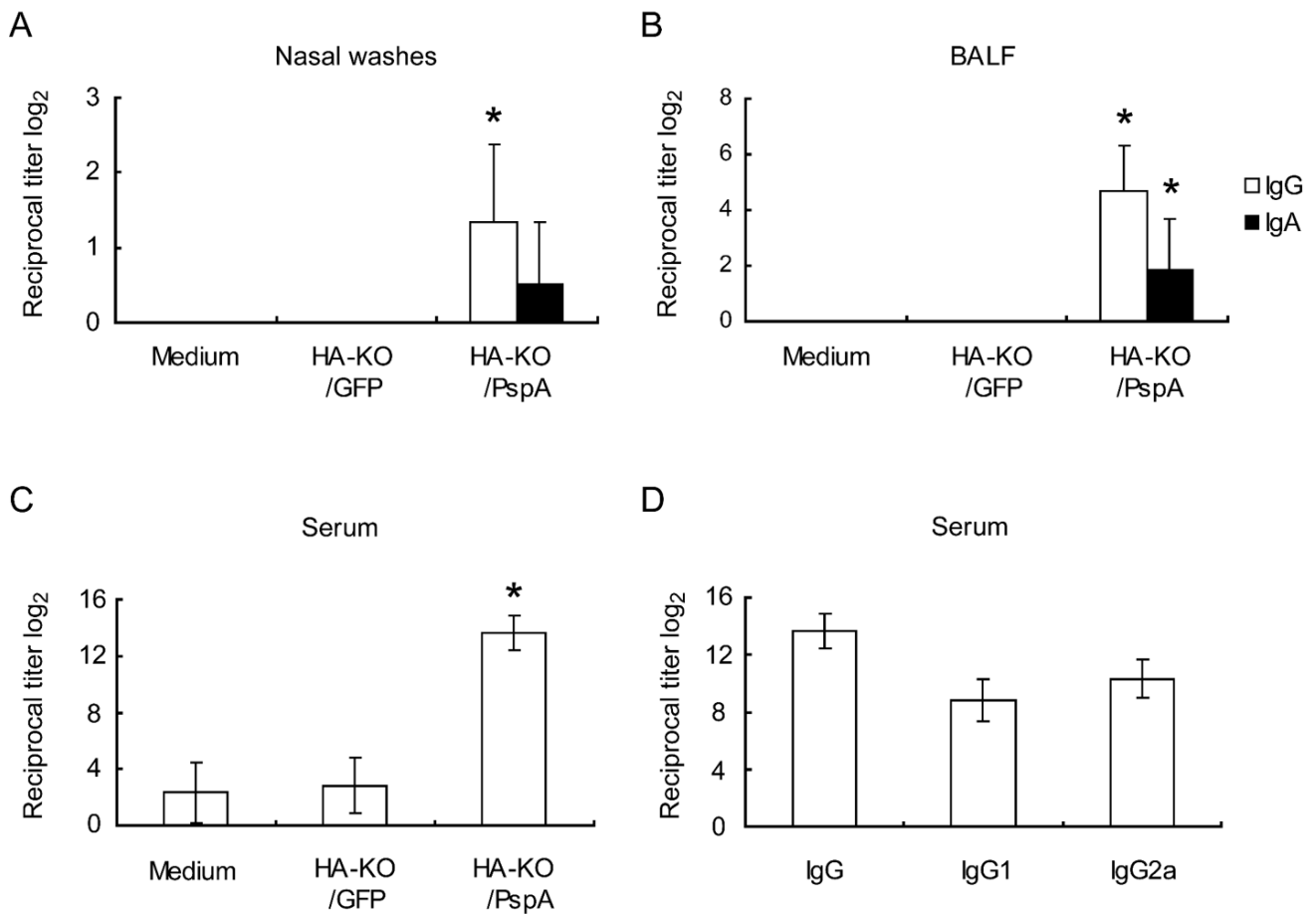
Fig. 3. Induction of PspA-specific IgG and IgA levels in nasal washes (A), and BALF (B), and IgG levels in serum (C), as well as IgG1 and IgG2a levels in serum.

Mice were intranasally inoculated with medium, HA-KO GFP virus, or HA-KO PspA virus with a two-weeks interval between the inoculations. Samples from six mice from each group were collected two weeks after the final vaccination. PspA-specific antibodies were detected by an ELISA. Results are expressed as the means of the reciprocal titer $\log_2$ (mean ± SD). Statistically significant differences between groups were determined by using the Dunnet method. The asterisk indicates a significant difference from samples taken from mice inoculated with medium (*, $P<0.05$).

Protective efficacy of HA-KO/PspA virus against lethal doses of *S. pneumoniae* and influenza virus. To evaluate the protective efficacy of HA-KO/PspA virus against *S. pneumoniae* and influenza virus, I performed a challenge experiment. Mice were intranasally inoculated with medium, HA-KO/GFP, or HA-KO/PspA virus on the same schedule as the aforementioned experiment. Two weeks after the final vaccination, these mice were infected with lethal doses of PR8 and *S. pneumoniae* serotype 3 strain WU2. Their body weight changes and survival were monitored during the observation period.

In the case of influenza virus infection, the body weights of mice inoculated with medium rapidly decreased and all mice died by day 5 after infection (Fig. 4). On the other hand, mice inoculated with either HA-KO/PspA or HA-KO/GFP virus showed no reduction in body weight and all of these mice survived during the observation period (Fig. 4). I also determined virus titers in the lungs and nasal turbinates of each group of mice after challenge (Table 1). Although virus was recovered from the lungs of 2 out of 3 mice inoculated with HA-KO/PspA virus on day 3 after challenge, virus titers were appreciably lower than those in the lungs of mice inoculated with medium. Further, except for the lungs of these mice, virus in the nasal turbinates and lungs of mice inoculated with HA-KO/PspA or HA-KO/GFP virus was undetectable on days 3 and 6 after challenge. These results indicate that the HA-KO/PspA and HA-KO/GFP viruses confer protective immunity to mice against a lethal dose of influenza virus.

As regards the *S. pneumoniae* infection, all mice inoculated with medium died. Moreover, in contrast to the PR8 infection, all mice inoculated with HA-KO/GFP virus also died. However, all mice inoculated with HA-KO/PspA virus survived (Fig. 5A). I also determined the level of bacterial colonization of the nasopharynx of each group of

mice. *S. pneumoniae* serotype 19F strain EF3030 was used in this experiment. Although the bacterial densities of the nasopharynx of mice inoculated with HA-KO/GFP virus was comparable to those of the nasopharynx of mice inoculated with medium, the bacterial densities of the nasopharynx of mice inoculated with HA-KO/PspA virus were significantly lower than those of the nasopharynx of mice inoculated with medium or HA-KO/GFP virus (Fig. 5B). These results indicate that HA-KO/PspA virus confers immunity against *S. pneumoniae* of a heterologous serotype because the PspA gene in HA-KO/PspA virus was derived from serotype 2 (strain Rx1) which is different from the serotype of the challenge bacterium (i.e., serotypes 3 and 19F).

Overall, these results demonstrate that HA-KO/PspA virus provides protective immunity to mice against lethal infection with influenza virus and *S. pneumoniae*, suggesting that HA-KO virus can be used as a platform for a bivalent vaccine against respiratory infectious diseases.

A   B
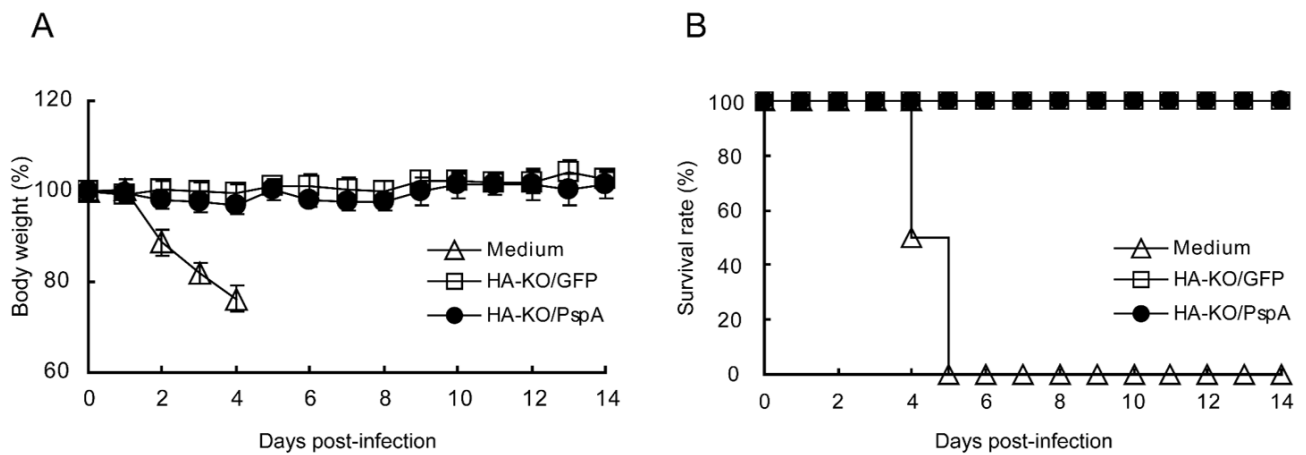
Fig. 4. Body weight changes and survival curves for mice challenged with lethal doses of PR8.

Eight mice per group were intranasally infected with 100 MLD$_{50}$ of PR8 two weeks after their final vaccination. Body weights were measured (A) and survival rate was monitored (B) for 14 days after infection. Open triangles (△), mice inoculated with medium; open squares (□), mice inoculated with HA-KO GFP virus; closed circles (●), mice inoculated with HA-KO PspA virus.
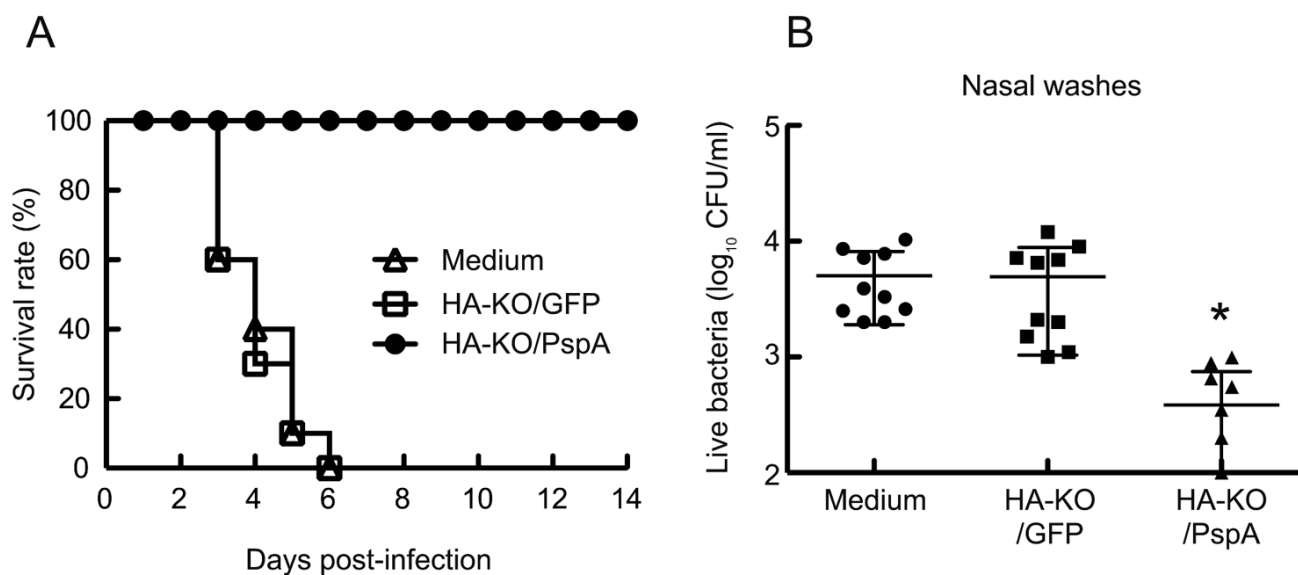
Fig. 5. Survival curves for mice challenged with lethal doses of *S. pneumoniae* WU2 strain, and bacterial densities in the nasopharynx 5 days after challenge with *S. pneumoniae* EF3030 strain.

(A) Ten mice per group were intranasally infected with 3 MLD_{50} of WU2 strain two weeks after their final vaccination. The survival rate was monitored for 14 days after infection. Open triangles (△), mice inoculated with medium; open squares (□), mice inoculated with HA-KO GFP virus; closed circles (●), mice inoculated with HA-KO PspA virus. (B) Mice were intranasally infected with 1 x 10^2 cfu/mouse of EF3030 strain two weeks after their final vaccination. Five days after challenge with EF3030 strain, nasal washes were collected, and a quantitative bacterial culture of nasal washes was performed. Values represent the log_{10} cfu/ml (mean $\pm$ SD) for ten mice per group. Closed circles (●), mice inoculated with medium; closed squares (■), mice inoculated with HA-KO GFP virus; closed triangles (▲), mice inoculated with HA-KO PspA virus. Statistically significant differences between groups were determined by using the Kaplan-Meier log-rank test for the survival analysis or the Mann-Whitney test for the bacterial clearance analysis. The asterisk indicates a significant difference (*, $P<0.05$).

85

Table 1. Protection against challenge with a lethal dose of PR8 in mice inoculated with HA-KO GFP or HA-KO PspA virus[a]

challenge dose	inoculum	days post-infection	organ	Virus titer (mean±SD log10[PFU/g])
100MLD$_{50}$	Medium	3dpi	NT[b]	6.3 ± 0.4
			Lung	7.9 ± 0.2
		6dpi	NT	NA[c]
			Lung	NA
	HA-KO GFP	3dpi	NT	ND[d]
			Lung	ND
		6dpi	NT	ND
			Lung	ND
	HA-KO PspA	3dpi	NT	ND
			Lung	2.9, 4.3
		6dpi	NT	ND
			Lung	ND

[a] Six mice from each group were intranasally infected with 100 MLD$_{50}$ of PR8 (50 μl per mouse) two weeks after the final vaccination. Three mice per group were sacrificed on days 3 and 6 post-infection, and lungs and nasal turbinate were collected to determine virus titers. Results are expressed as the mean titer (log$_{10}$ PFU/g)±standard deviations (SD). When virus was not recovered from all three mice, individual titers are given.

[b] NT: Nasal turbinate

[c] NA: Not applicable because the mice died

[d] ND: Not detected (detection limit, 10 PFU/lung or 5 PFU/NT)

Discussion

Secondary bacterial infections after influenza virus infections complicate disease severity and increase mortality and morbidity. Indeed, most victims of the 1918–19 influenza virus pandemic likely died from secondary bacterial pneumonia (Morens et al., 2008). In addition, autopsy samples from those who succumbed to infection with the 2009 pandemic H1N1 influenza virus exhibited signs of secondary bacterial infections, and the severity of the infections caused by this influenza virus was correlated with *S. pneumoniae* coinfection (Gill et al., 2010; Palacios et al., 2009). Damage to mucosal epithelial cells, exposure of receptors that facilitate bacterial adherence, and dysfunction of immune effectors by influenza virus infection are prominent features that allow bacteria access to the lower respiratory tract (McCullers et al., 2006). It was, thus, once thought that pneumococcal disease could be prevented by administering influenza vaccine alone because if the influenza virus infection was prevented, the above-described features that contribute to bacterial invasion would be minimized (Chaussee et al., 2011; Huber et al., 2010). However, such complete protection from bacterial infections through influenza vaccination alone is unlikely because of the lack of specific immunity against the bacteria. Therefore, the induction of antibodies against *S. pneumoniae* via vaccination is important to prevent such bacterial infections. Here, I generated a replication-incompetent HA-KO virus that encodes the PspA antigenic region in the coding region of its HA segment (HA-KO/PspA virus). This virus induced not only influenza virus- but also PspA-specific antibodies on the respiratory mucosa and in the sera of mice. I also demonstrated that mice inoculated with HA-KO/PspA virus were completely protected from lethal challenge with both *S. pneumoniae* and influenza virus. Therefore, my

findings suggest that HA-KO/PspA virus is a promising bivalent vaccine against both *S. pneumoniae* and influenza virus.

It has been previously demonstrated that intranasal administration of the PspA protein alone does not elicit an adequate antibody response and that administration of PspA with adjuvants, such as different types of TLR ligands, can confer sufficient immunity against *S. pneumoniae* in mice (Oma et al., 2009). Remarkably, however, I demonstrated that HA-KO/PspA virus induced efficient immunity against *S. pneumoniae* infection without any mucosal adjuvants. The possible mechanisms are as follows: first, infection with HA-KO/PspA virus triggers the innate immune response via recognition of vRNAs by pattern-recognition receptors, such as TLR7 (Diebold et al., 2004) and Retinoic acid-inducible gene-I (RIG-I) (Hornung et al ., 2006; Pichlmair et al ., 2006), in the infected cells since these vRNAs are amplified in HA-KO/PspA virus-infected cells even though infectious progeny virus cannot be generated; second, PspA is expressed in virus-infected cells as shown in Fig, 1; and third, antigen-presenting cells (APCs) phagocytose the infected cells that contain the ligands for the TLRs (vRNAs) and the antigens (PspA besides viral proteins), and the major histocompatibility complex classes I and II efficiently present these antigens on the cell surface of the APCs (Blander et al., 2006; Schulz et al., 2005). As such, it is possible for PspA-specific antibodies to be induced by HA-KO/PspA virus in the absence of any exogenous mucosal adjuvants.

In conclusion, the replication-incompetent influenza virus-based approach presented here could be used as a platform to develop bivalent vaccine candidates against various pathogens that cause respiratory infectious diseases.

CONCLUDING REMARKS

Influenza viruses cause epidemics and occasional pandemics. Since the beginning of the 20th century, we have experienced four pandemics (Wright et al., 2013). In addition, sporadic infections caused by H5N1 and H7N9 viruses have been reported in recent years. Despite advances in medicine and the availability of new antivirals, influenza viruses continue to be a great threat to our lives. To develop novel antivirals and vaccines to control influenza, we must continue to conduct basic research on influenza virus infection. In this thesis, I focused on host responses to influenza virus infection and novel vaccine production based on genetic recombination technology of influenza virus.

In chapter I, I characterized an improved recombinant influenza A virus carrying a reporter gene (NS1-Venus PR8 MA virus). I demonstrated that NS1-Venus PR8 MA virus stably expressed the Venus protein at high levels. By using NS1-Venus PR8 MA virus, I could readily detect virus-infected cells. I believe that NS1-Venus PR8 MA virus could be useful not only in intravital live imaging experiments, which has not been successful to date, but also in screens for new antivirals.

Vaccination is effective in the prophylaxis of influenza virus infection. However, there is still room for improvement in the efficacy and safety of our current vaccines. In chapter II, I generated a replication-incompetent influenza virus that lacks membrane-fusion ability to evaluate as an influenza vaccine. I demonstrated that mice inoculated with this uncleavable HA virus could successfully elicit not only virus-specific antibodies at the surface of respiratory mucosa but also cytotoxic T lymphocytes in the lung. I also showed that the uncleavable HA virus completely protected mice from lethal infection with influenza virus.

On the basis of the results described in chapter II, in chapter III, I generated a bivalent vaccine designed to protect against influenza virus and *S. pneumoniae* infection. By using the packaging signal of the HA segment, I produced HA-KO/PspA virus, which expresses PspA protein as an antigen of *S. pneumoniae* in infected cells. I demonstrated that HA-KO/PspA virus could prevent nasal colonization and lethal infection due to *S. pneumoniae* as well as lethal infection by influenza virus. Therefore I believe that a replication-incompetent virus can serve as a bivalent vaccine.

Despite the intense efforts of influenza virus researchers, several important problems remain, including the emergence of antiviral-resistant viruses and inefficient influenza vaccines. Moreover, we cannot predict which subtype of virus will cause the next pandemic. To better understand influenza virus, we must continuously conduct intensive basic research. I hope that the results presented here will contribute to the elucidation of the pathogenesis of influenza virus and help establish new prophylactic and therapeutic measures to control influenza virus infection.

ACKNOWLEDGEMENTS

REFERENCES

Ambrose CS, Luke C, Coelingh K. 2008. Current status of live attenuated influenza vaccine in the United States for seasonal and pandemic influenza. Influenza Other Respi Viruses **2:**193-202.

Baskin CR, Bielefeldt-Ohmann H, Tumpey TM, Sabourin PJ, Long JP, García-Sastre A, Tolnay AE, Albrecht R, Pyles JA, Olson PH, Aicher LD, Rosenzweig ER, Murali-Krishna K, Clark EA, Kotur MS, Fornek JL, Proll S, Palermo RE, Sabourin CL, Katze MG. 2009. Early and sustained innate immune response defines pathology and death in nonhuman primates infected by highly pathogenic influenza virus. Proc Natl Acad Sci U S A **106:**3455-3460.

Belser JA, Gustin KM, Pearce MB, Maines TR, Zeng H, Pappas C, Sun X, Carney PJ, Villanueva JM, Stevens J, Katz JM, Tumpey TM. 2013. Pathogenesis and transmission of avian influenza A (H7N9) virus in ferrets and mice. Nature **501:**556-559.

Bettelli E, Das MP, Howard ED, Weiner HL, Sobel RA, Kuchroo VK. 1998. IL-10 is critical in the regulation of autoimmune encephalomyelitis as demonstrated by studies of IL-10- and IL-4-deficient and transgenic mice. J Immunol **161:**3299-3306.

Blander JM, Medzhitov R. 2006. Toll-dependent selection of microbial antigens for presentation by dendritic cells. Nature **440:**808-812.

Bogaert D, De Groot R, Hermans PW. 2004. Streptococcus pneumoniae colonisation: the key to pneumococcal disease. Lancet Infect Dis **4:**144-154.

Briles DE, Hollingshead SK, Paton JC, Ades EW, Novak L, van Ginkel FW, Benjamin WH. 2003. Immunizations with pneumococcal surface protein A and pneumolysin are protective against pneumonia in a murine model of pulmonary infection with Streptococcus pneumoniae. J Infect Dis **188:**339-348.

Briles DE, Novak L, Hotomi M, van Ginkel FW, King J. 2005. Nasal colonization with Streptococcus pneumoniae includes subpopulations of surface and invasive pneumococci. Infect Immun **73:**6945-6951.

Chaussee MS, Sandbulte HR, Schuneman MJ, Depaula FP, Addengast LA, Schlenker EH, Huber VC. 2011. Inactivated and live, attenuated influenza vaccines protect mice against influenza: Streptococcus pyogenes super-infections. Vaccine **29:**3773-3781.

Chen Y, Liang W, Yang S, Wu N, Gao H, Sheng J, Yao H, Wo J, Fang Q, Cui D, Li Y, Yao X, Zhang Y, Wu H, Zheng S, Diao H, Xia S, Chan KH, Tsoi HW, Teng JL, Song W, Wang P, Lau SY, Zheng M, Chan JF, To KK, Chen H, Li L, Yuen KY. 2013. Human infections with the emerging avian influenza A H7N9 virus from wet market poultry: clinical analysis and characterisation of viral genome. Lancet **381:**1916-1925.

Chen Z, Aspelund A, Kemble G, Jin H. 2006. Genetic mapping of the cold-adapted phenotype of B/Ann Arbor/1/66, the master donor virus for live attenuated influenza vaccines (FluMist). Virology **345:**416-423.

Claas EC, Osterhaus AD, van Beek R, De Jong JC, Rimmelzwaan GF, Senne DA, Krauss S, Shortridge KF, Webster RG. 1998. Human influenza A H5N1 virus related to a highly pathogenic avian influenza virus. Lancet **351:**472-477.

Cox RJ, Brokstad KA, Ogra P. 2004. Influenza virus: immunity and vaccination strategies. Comparison of the immune response to inactivated and live, attenuated influenza vaccines. Scand J Immunol **59:**1-15.

Dawood FS, Jain S, Finelli L, Shaw MW, Lindstrom S, Garten RJ, Gubareva LV, Xu X, Bridges CB, Uyeki TM, Novel Swine-Origin Influenza A (H1N1) Virus Investigation Team. 2009. Emergence of a novel swine-origin influenza A (H1N1) virus in humans. N Engl J Med **360:**2605-2615.

de Jong MD, Simmons CP, Thanh TT, Hien VM, Smith GJ, Chau TN, Hoang DM, Chau NV, Khanh TH, Dong VC, Qui PT, Cam BV, Ha dQ, Guan Y, Peiris JS, Chinh NT, Hien TT, Farrar J. 2006. Fatal outcome of human influenza A (H5N1) is associated with high viral load and hypercytokinemia. Nat Med **12:**1203-1207.

Diebold SS, Kaisho T, Hemmi H, Akira S, Reis e Sousa C. 2004. Innate antiviral

responses by means of TLR7-mediated recognition of single-stranded RNA. Science **303:**1529-1531.

Do-Umehara HC, Chen C, Urich D, Zhou L, Qiu J, Jang S, Zander A, Baker MA, Eilers M, Sporn PH, Ridge KM, Sznajder JI, Budinger GR, Mutlu GM, Lin A, Liu J. 2013. Suppression of inflammation and acute lung injury by Miz1 via repression of C/EBP-δ. Nat Immunol **14:**461-469.

Ezoe H, Akeda Y, Piao Z, Aoshi T, Koyama S, Tanimoto T, Ishii KJ, Oishi K. 2011. Intranasal vaccination with pneumococcal surface protein A plus poly(I:C) protects against secondary pneumococcal pneumonia in mice. Vaccine **29:**1754-1761.

Ferreira DM, Darrieux M, Oliveira ML, Leite LC, Miyaji EN. 2008. Optimized immune response elicited by a DNA vaccine expressing pneumococcal surface protein a is characterized by a balanced immunoglobulin G1 (IgG1)/IgG2a ratio and proinflammatory cytokine production. Clin Vaccine Immunol **15:**499-505.

Fiore AE, Uyeki TM, Broder K, Finelli L, Euler GL, Singleton JA, Iskander JK, Wortley PM, Shay DK, Bresee JS, Cox NJ. 2010. Prevention and control of influenza with vaccines: recommendations of the Advisory Committee on Immunization Practices (ACIP), 2010. MMWR Recomm Rep **59:**1-62.

Gabriel G, Dauber B, Wolff T, Planz O, Klenk HD, Stech J. 2005. The viral polymerase mediates adaptation of an avian influenza virus to a mammalian host. Proc

Natl Acad Sci U S A **102:**18590-18595.

Gao R, Cao B, Hu Y, Feng Z, Wang D, Hu W, Chen J, Jie Z, Qiu H, Xu K, Xu X,
Lu H, Zhu W, Gao Z, Xiang N, Shen Y, He Z, Gu Y, Zhang Z, Yang Y, Zhao X,
Zhou L, Li X, Zou S, Zhang Y, Yang L, Guo J, Dong J, Li Q, Dong L, Zhu Y, Bai
T, Wang S, Hao P, Yang W, Han J, Yu H, Li D, Gao GF, Wu G, Wang Y, Yuan Z,
Shu Y.** 2013. Human infection with a novel avian-origin influenza A (H7N9) virus. N
Engl J Med **368:**1888-1897.

Gill JR, Sheng ZM, Ely SF, Guinee DG, Beasley MB, Suh J, Deshpande C, Mollura
DJ, Morens DM, Bray M, Travis WD, Taubenberger JK.** 2010. Pulmonary
pathologic findings of fatal 2009 pandemic influenza A/H1N1 viral infections. Arch
Pathol Lab Med **134:**235-243.

Gorai T, Goto H, Noda T, Watanabe T, Kozuka-Hata H, Oyama M, Takano R,
Neumann G, Watanabe S, Kawaoka Y.** 2012. F1Fo-ATPase, F-type proton-
translocating ATPase, at the plasma membrane is critical for efficient influenza virus
budding. Proc Natl Acad Sci U S A **109:**4615-4620.

Gruenberg DA, Shaker MS.** 2011. An update on influenza vaccination in patients with
egg allergy. Curr Opin Pediatr **23:**566-572.

Hama H, Kurokawa H, Kawano H, Ando R, Shimogori T, Noda H, Fukami K,
Sakaue-Sawano A, Miyawaki A.** 2011. Scale: a chemical approach for fluorescence

imaging and reconstruction of transparent mouse brain. Nat Neurosci **14:**1481-1488.

Hatta M, Gao P, Halfmann P, Kawaoka Y. 2001. Molecular basis for high virulence of Hong Kong H5N1 influenza A viruses. Science **293:**1840-1842.

Hatta M, Hatta Y, Kim JH, Watanabe S, Shinya K, Nguyen T, Lien PS, Le QM, Kawaoka Y. 2007. Growth of H5N1 influenza A viruses in the upper respiratory tracts of mice. PLoS Pathog **3:**1374-1379.

Herfst S, Schrauwen EJ, Linster M, Chutinimitkul S, de Wit E, Munster VJ, Sorrell EM, Bestebroer TM, Burke DF, Smith DJ, Rimmelzwaan GF, Osterhaus AD, Fouchier RA. 2012. Airborne transmission of influenza A/H5N1 virus between ferrets. Science **336:**1534-1541.

Hoffmann E, Mahmood K, Chen Z, Yang CF, Spaete J, Greenberg HB, Herlocher ML, Jin H, Kemble G. 2005. Multiple gene segments control the temperature sensitivity and attenuation phenotypes of ca B/Ann Arbor/1/66. J Virol **79:**11014-11021.

Horimoto T, Murakami S, Muramoto Y, Yamada S, Fujii K, Kiso M, Iwatsuki-Horimoto K, Kino Y, Kawaoka Y. 2007. Enhanced growth of seed viruses for H5N1 influenza vaccines. Virology **366:**23-27.

Hornung V, Ellegast J, Kim S, Brzózka K, Jung A, Kato H, Poeck H, Akira S,

Conzelmann KK, Schlee M, Endres S, Hartmann G. 2006. 5'-Triphosphate RNA is the ligand for RIG-I. Science **314:**994-997.

Huber VC, Peltola V, Iverson AR, McCullers JA. 2010. Contribution of vaccine-induced immunity toward either the HA or the NA component of influenza viruses limits secondary bacterial complications. J Virol **84:**4105-4108.

Imai M, Watanabe T, Hatta M, Das SC, Ozawa M, Shinya K, Zhong G, Hanson A, Katsura H, Watanabe S, Li C, Kawakami E, Yamada S, Kiso M, Suzuki Y, Maher EA, Neumann G, Kawaoka Y. 2012. Experimental adaptation of an influenza H5 HA confers respiratory droplet transmission to a reassortant H5 HA/H1N1 virus in ferrets. Nature **486:**420-428.

Iwasaki A. 2012. A virological view of innate immune recognition. Annu Rev Microbiol **66:**177-196.

Jambo KC, Sepako E, Heyderman RS, Gordon SB. 2010. Potential role for mucosally active vaccines against pneumococcal pneumonia. Trends Microbiol **18:**81-89.

Jedrzejas MJ. 2007. Unveiling molecular mechanisms of bacterial surface proteins: Streptococcus pneumoniae as a model organism for structural studies. Cell Mol Life Sci **64:**2799-2822.

Jin H, Lu B, Zhou H, Ma C, Zhao J, Yang CF, Kemble G, Greenberg H. 2003. Multiple amino acid residues confer temperature sensitivity to human influenza virus vaccine strains (FluMist) derived from cold-adapted A/Ann Arbor/6/60. Virology **306:**18-24.

Jin H, Zhou H, Lu B, Kemble G. 2004. Imparting temperature sensitivity and attenuation in ferrets to A/Puerto Rico/8/34 influenza virus by transferring the genetic signature for temperature sensitivity from cold-adapted A/Ann Arbor/6/60. J Virol **78:**995-998.

Joller N, Hafler JP, Brynedal B, Kassam N, Spoerl S, Levin SD, Sharpe AH, Kuchroo VK. 2011. Cutting edge: TIGIT has T cell-intrinsic inhibitory functions. J Immunol **186:**1338-1342.

Kadioglu A, Weiser JN, Paton JC, Andrew PW. 2008. The role of Streptococcus pneumoniae virulence factors in host respiratory colonization and disease. Nat Rev Microbiol **6:**288-301.

Katsura H, Iwatsuki-Horimoto K, Fukuyama S, Watanabe S, Sakabe S, Hatta Y, Murakami S, Shimojima M, Horimoto T, Kawaoka Y. 2012. A replication-incompetent virus possessing an uncleavable hemagglutinin as an influenza vaccine. Vaccine **30:**6027-6033.

Katz JM, Naeve CW, Webster RG. 1987. Host cell-mediated variation in H3N2

influenza viruses. Virology **156:**386-395.

Katz JM, Wang M, Webster RG. 1990. Direct sequencing of the HA gene of influenza (H3N2) virus in original clinical samples reveals sequence identity with mammalian cell-grown virus. J Virol **64:**1808-1811.

Katz JM, Webster RG. 1989. Efficacy of inactivated influenza A virus (H3N2) vaccines grown in mammalian cells or embryonated eggs. J Infect Dis **160:**191-198.

Kawai T, Akira S. 2006. Innate immune recognition of viral infection. Nat Immunol **7:**131-137.

Kawamoto S, Tran TH, Maruya M, Suzuki K, Doi Y, Tsutsui Y, Kato LM, Fagarasan S. 2012. The inhibitory receptor PD-1 regulates IgA selection and bacterial composition in the gut. Science **336:**485-489.

Kawaoka Y, Krauss S, Webster RG. 1989. Avian-to-human transmission of the PB1 gene of influenza A viruses in the 1957 and 1968 pandemics. J Virol **63:**4603-4608.

Keir ME, Butte MJ, Freeman GJ, Sharpe AH. 2008. PD-1 and its ligands in tolerance and immunity. Annu Rev Immunol **26:**677-704.

Kida H, Brown LE, Webster RG. 1982. Biological activity of monoclonal antibodies to operationally defined antigenic regions on the hemagglutinin molecule of

A/Seal/Massachusetts/1/80 (H7N7) influenza virus. Virology **122:**38-47.

King C, Tangye SG, Mackay CR. 2008. T follicular helper (TFH) cells in normal and dysregulated immune responses. Annu Rev Immunol **26:**741-766.

Kittel C, Sereinig S, Ferko B, Stasakova J, Romanova J, Wolkerstorfer A, Katinger H, Egorov A. 2004. Rescue of influenza virus expressing GFP from the NS1 reading frame. Virology **324:**67-73.

Kobasa D, Jones SM, Shinya K, Kash JC, Copps J, Ebihara H, Hatta Y, Kim JH, Halfmann P, Hatta M, Feldmann F, Alimonti JB, Fernando L, Li Y, Katze MG, Feldmann H, Kawaoka Y. 2007. Aberrant innate immune response in lethal infection of macaques with the 1918 influenza virus. Nature **445:**319-323.

Kühn R, Löhler J, Rennick D, Rajewsky K, Müller W. 1993. Interleukin-10-deficient mice develop chronic enterocolitis. Cell **75:**263-274.

La Gruta NL, Kedzierska K, Stambas J, Doherty PC. 2007. A question of self-preservation: immunopathology in influenza virus infection. Immunol Cell Biol **85:**85-92.

Lambert LC, Fauci AS. 2010. Influenza vaccines for the future. N Engl J Med **363:**2036-2044.

Li Q, Zhou L, Zhou M, Chen Z, Li F, Wu H, Xiang N, Chen E, Tang F, Wang D, Meng L, Hong Z, Tu W, Cao Y, Li L, Ding F, Liu B, Wang M, Xie R, Gao R, Li X, Bai T, Zou S, He J, Hu J, Xu Y, Chai C, Wang S, Gao Y, Jin L, Zhang Y, Luo H, Yu H, Gao L, Pang X, Liu G, Shu Y, Yang W, Uyeki TM, Wang Y, Wu F, Feng Z. 2013. Preliminary Report: Epidemiology of the Avian Influenza A (H7N9) Outbreak in China. N Engl J Med.

Li Z, Chen H, Jiao P, Deng G, Tian G, Li Y, Hoffmann E, Webster RG, Matsuoka Y, Yu K. 2005. Molecular basis of replication of duck H5N1 influenza viruses in a mammalian mouse model. J Virol **79:**12058-12064.

Lozach PY, Huotari J, Helenius A. 2011. Late-penetrating viruses. Curr Opin Virol **1:**35-43.

Maassab HF. 1968. Plaque formation of influenza virus at 25 degrees C. Nature **219:**645-646.

Manicassamy B, Manicassamy S, Belicha-Villanueva A, Pisanelli G, Pulendran B, García-Sastre A. 2010. Analysis of in vivo dynamics of influenza virus infection in mice using a GFP reporter virus. Proc Natl Acad Sci U S A **107:**11531-11536.

Mantovani A, Biswas SK, Galdiero MR, Sica A, Locati M. 2013. Macrophage plasticity and polarization in tissue repair and remodelling. J Pathol **229:**176-185.

Martin K, Helenius A. 1991. Nuclear transport of influenza virus ribonucleoproteins: the viral matrix protein (M1) promotes export and inhibits import. Cell **67:**117-130.

Matlin KS, Reggio H, Helenius A, Simons K. 1981. Infectious entry pathway of influenza virus in a canine kidney cell line. J Cell Biol **91:**601-613.

McCullers JA. 2006. Insights into the interaction between influenza virus and pneumococcus. Clin Microbiol Rev **19:**571-582.

Moffitt KL, Malley R. 2011. Next generation pneumococcal vaccines. Curr Opin Immunol **23:**407-413.

Morens DM, Taubenberger JK, Fauci AS. 2008. Predominant role of bacterial pneumonia as a cause of death in pandemic influenza: implications for pandemic influenza preparedness. J Infect Dis **198:**962-970.

Nabors GS, Braun PA, Herrmann DJ, Heise ML, Pyle DJ, Gravenstein S, Schilling M, Ferguson LM, Hollingshead SK, Briles DE, Becker RS. 2000. Immunization of healthy adults with a single recombinant pneumococcal surface protein A (PspA) variant stimulates broadly cross-reactive antibodies to heterologous PspA molecules. Vaccine **18:**1743-1754.

Nagai T, Ibata K, Park ES, Kubota M, Mikoshiba K, Miyawaki A. 2002. A variant of yellow fluorescent protein with fast and efficient maturation for cell-biological

applications. Nat Biotechnol **20:**87-90.

Narasaraju T, Yang E, Samy RP, Ng HH, Poh WP, Liew AA, Phoon MC, van Rooijen N, Chow VT. 2011. Excessive neutrophils and neutrophil extracellular traps contribute to acute lung injury of influenza pneumonitis. Am J Pathol **179:**199-210.

Neumann G, Noda T, Kawaoka Y. 2009. Emergence and pandemic potential of swine-origin H1N1 influenza virus. Nature **459:**931-939.

Neumann G, Watanabe T, Ito H, Watanabe S, Goto H, Gao P, Hughes M, Perez DR, Donis R, Hoffmann E, Hobom G, Kawaoka Y. 1999. Generation of influenza A viruses entirely from cloned cDNAs. Proc Natl Acad Sci U S A **96:**9345-9350.

Newman RW, Jennings R, Major DL, Robertson JS, Jenkins R, Potter CW, Burnett I, Jewes L, Anders M, Jackson D. 1993. Immune response of human volunteers and animals to vaccination with egg-grown influenza A (H1N1) virus is influenced by three amino acid substitutions in the haemagglutinin molecule. Vaccine **11:**400-406.

Niwa H, Yamamura K, Miyazaki J. 1991. Efficient selection for high-expression transfectants with a novel eukaryotic vector. Gene **108:**193-199.

Ochs MM, Bartlett W, Briles DE, Hicks B, Jurkuvenas A, Lau P, Ren B, Millar A. 2008. Vaccine-induced human antibodies to PspA augment complement C3 deposition

on Streptococcus pneumoniae. Microb Pathog **44:**204-214.

Oma K, Zhao J, Ezoe H, Akeda Y, Koyama S, Ishii KJ, Kataoka K, Oishi K. 2009. Intranasal immunization with a mixture of PspA and a Toll-like receptor agonist induces specific antibodies and enhances bacterial clearance in the airways of mice. Vaccine **27:**3181-3188.

Ouyang W, Rutz S, Crellin NK, Valdez PA, Hymowitz SG. 2011. Regulation and functions of the IL-10 family of cytokines in inflammation and disease. Annu Rev Immunol **29:**71-109.

Palacios G, Hornig M, Cisterna D, Savji N, Bussetti AV, Kapoor V, Hui J, Tokarz R, Briese T, Baumeister E, Lipkin WI. 2009. Streptococcus pneumoniae coinfection is correlated with the severity of H1N1 pandemic influenza. PLoS One **4:**e8540.

Pichlmair A, Schulz O, Tan CP, Näslund TI, Liljeström P, Weber F, Reis e Sousa C. 2006. RIG-I-mediated antiviral responses to single-stranded RNA bearing 5'-phosphates. Science **314:**997-1001.

Rawlins EL, Hogan BL. 2006. Epithelial stem cells of the lung: privileged few or opportunities for many? Development **133:**2455-2465.

Ren B, Szalai AJ, Hollingshead SK, Briles DE. 2004. Effects of PspA and antibodies to PspA on activation and deposition of complement on the pneumococcal surface.

Infect Immun **72:**114-122.

Richard M, Schrauwen EJ, de Graaf M, Bestebroer TM, Spronken MI, van Boheemen S, de Meulder D, Lexmond P, Linster M, Herfst S, Smith DJ, van den Brand JM, Burke DF, Kuiken T, Rimmelzwaan GF, Osterhaus AD, Fouchier RA. 2013. Limited airborne transmission of H7N9 influenza A virus between ferrets. Nature **501:**560-563.

Rimmelzwaan GF, Fouchier RA, Osterhaus AD. 2007. Influenza virus-specific cytotoxic T lymphocytes: a correlate of protection and a basis for vaccine development. Curr Opin Biotechnol **18:**529-536.

Rodgers GL, Klugman KP. 2011. The future of pneumococcal disease prevention. Vaccine **29 Suppl 3:**C43-48.

Rogers GN, Paulson JC. 1983. Receptor determinants of human and animal influenza virus isolates: differences in receptor specificity of the H3 hemagglutinin based on species of origin. Virology **127:**361-373.

Sakabe S, Ozawa M, Takano R, Iwastuki-Horimoto K, Kawaoka Y. 2011. Mutations in PA, NP, and HA of a pandemic (H1N1) 2009 influenza virus contribute to its adaptation to mice. Virus Res **158:**124-129.

Saraiva M, O'Garra A. 2010. The regulation of IL-10 production by immune cells.

Nat Rev Immunol **10:**170-181.

Scholtissek C, Rohde W, Von Hoyningen V, Rott R. 1978. On the origin of the human influenza virus subtypes H2N2 and H3N2. Virology **87:**13-20.

Schulz O, Diebold SS, Chen M, Näslund TI, Nolte MA, Alexopoulou L, Azuma YT, Flavell RA, Liljeström P, Reis e Sousa C. 2005. Toll-like receptor 3 promotes cross-priming to virus-infected cells. Nature **433:**887-892.

Shinya K, Fujii Y, Ito H, Ito T, Kawaoka Y. 2004. Characterization of a neuraminidase-deficient influenza a virus as a potential gene delivery vector and a live vaccine. J Virol **78:**3083-3088.

Short KR, Kroeze EJ, Fouchier RA, Kuiken T. 2013. Pathogenesis of influenza-induced acute respiratory distress syndrome. Lancet Infect Dis. (in press)

Sica A, Mantovani A. 2012. Macrophage plasticity and polarization: in vivo veritas. J Clin Invest **122:**787-795.

Sieczkarski SB, Whittaker GR. 2002. Influenza virus can enter and infect cells in the absence of clathrin-mediated endocytosis. J Virol **76:**10455-10464.

Skehel JJ, Wiley DC. 2000. Receptor binding and membrane fusion in virus entry: the influenza hemagglutinin. Annu Rev Biochem **69:**531-569.

Smith GJ, Vijaykrishna D, Bahl J, Lycett SJ, Worobey M, Pybus OG, Ma SK, Cheung CL, Raghwani J, Bhatt S, Peiris JS, Guan Y, Rambaut A. 2009. Origins and evolutionary genomics of the 2009 swine-origin H1N1 influenza A epidemic. Nature 459:1122-1125.

Snelgrove RJ, Godlee A, Hussell T. 2011. Airway immune homeostasis and implications for influenza-induced inflammation. Trends Immunol **32:**328-334.

Snelgrove RJ, Goulding J, Didierlaurent AM, Lyonga D, Vekaria S, Edwards L, Gwyer E, Sedgwick JD, Barclay AN, Hussell T. 2008. A critical function for CD200 in lung immune homeostasis and the severity of influenza infection. Nat Immunol **9:**1074-1083.

Teijaro JR, Walsh KB, Cahalan S, Fremgen DM, Roberts E, Scott F, Martinborough E, Peach R, Oldstone MB, Rosen H. 2011. Endothelial cells are central orchestrators of cytokine amplification during influenza virus infection. Cell **146:**980-991.

Tong S, Li Y, Rivailler P, Conrardy C, Castillo DA, Chen LM, Recuenco S, Ellison JA, Davis CT, York IA, Turmelle AS, Moran D, Rogers S, Shi M, Tao Y, Weil MR, Tang K, Rowe LA, Sammons S, Xu X, Frace M, Lindblade KA, Cox NJ, Anderson LJ, Rupprecht CE, Donis RO. 2012. A distinct lineage of influenza A virus from bats. Proc Natl Acad Sci U S A **109:**4269-4274.

Tong S, Zhu X, Li Y, Shi M, Zhang J, Bourgeois M, Yang H, Chen X, Recuenco S, Gomez J, Chen LM, Johnson A, Tao Y, Dreyfus C, Yu W, McBride R, Carney PJ, Gilbert AT, Chang J, Guo Z, Davis CT, Paulson JC, Stevens J, Rupprecht CE, Holmes EC, Wilson IA, Donis RO. 2013. New world bats harbor diverse influenza A viruses. PLoS Pathog **9:**e1003657.

Wang J, Li F, Sun R, Gao X, Wei H, Li LJ, Tian Z. 2013. Bacterial colonization dampens influenza-mediated acute lung injury via induction of M2 alveolar macrophages. Nat Commun **4:**2106.

Watanabe T, Kiso M, Fukuyama S, Nakajima N, Imai M, Yamada S, Murakami S, Yamayoshi S, Iwatsuki-Horimoto K, Sakoda Y, Takashita E, McBride R, Noda T, Hatta M, Imai H, Zhao D, Kishida N, Shirakura M, de Vries RP, Shichinohe S, Okamatsu M, Tamura T, Tomita Y, Fujimoto N, Goto K, Katsura H, Kawakami E, Ishikawa I, Watanabe S, Ito M, Sakai-Tagawa Y, Sugita Y, Uraki R, Yamaji R, Eisfeld AJ, Zhong G, Fan S, Ping J, Maher EA, Hanson A, Uchida Y, Saito T, Ozawa M, Neumann G, Kida H, Odagiri T, Paulson JC, Hasegawa H, Tashiro M, Kawaoka Y. 2013. Characterization of H7N9 influenza A viruses isolated from humans. Nature **501:**551-555.

Watanabe T, Watanabe S, Neumann G, Kida H, Kawaoka Y. 2002. Immunogenicity and protective efficacy of replication-incompetent influenza virus-like particles. J Virol **76:**767-773.

Watanabe T, Watanabe S, Noda T, Fujii Y, Kawaoka Y. 2003. Exploitation of

nucleic acid packaging signals to generate a novel influenza virus-based vector stably

expressing two foreign genes. J Virol **77:**10575-10583.

Williams SP, Robertson JS. 1993. Analysis of the restriction to the growth of nonegg-

adapted human influenza virus in eggs. Virology **196:**660-665.

Wright P, Neumann G, Kawaoka Y. 2013. Orthomyxoviruses, Fields Virology 6th

edition

(Lippincott Williams & Wilkins).

**Yu X, Harden K, Gonzalez LC, Francesco M, Chiang E, Irving B, Tom I, Ivelja S,

Refino CJ, Clark H, Eaton D, Grogan JL.** 2009. The surface protein TIGIT

suppresses T cell activation by promoting the generation of mature immunoregulatory

dendritic cells. Nat Immunol **10:**48-57.